Wegener, Christoph; Kruse-Becher, Robinson; Klein, Tony

Conference Paper

EU ETS Market Expectations and Rational Bubbles

Beiträge zur Jahrestagung des Vereins für Socialpolitik 2024: Upcoming Labor Market Challenges

Provided in Cooperation with:
Verein für Socialpolitik / German Economic Association

EU ETS Market Expectations and Rational Bubbles

Christoph Wegener
Leuphana University Lüneburg, School of Management and Technology
Center for Methods
Universitätsallee 1, 21335 Lüneburg, Germany
christoph.wegener@leuphana.de
Robinson Kruse-Becher
University of Hagen, Faculty of Business Administration and Economics
Center for Economic and Statistical Analysis (CESA)
Universitätsstr. 41, 58097 Hagen, Germany
robinson.kruse-becher@fernuni-hagen.de
Tony Klein
Queen's University Belfast, Queen's Management School
Riddel Hall, 185 Stranmillis Road, Belfast BT9 5EE, UK
Technische Universität Chemnitz, Faculty of Business and Economics
Thüringer Weg 7, 09126 Chemnitz, Germany
tony.klein@wiwi.tu-chemnitz.de

February 17, 2024

EU ETS Market Expectations and Rational Bubbles

Abstract

Concerns about a price bubble within the European Union Emissions Trading System (EU ETS) emerged during the third trading period. We argue that bubble tests based on costs for switching from cheap, polluting to costly, clean energy sources is restricted to situations of market certainty. This limitation is unrealistic, considering the ongoing CO_2 reduction measures. Additionally, establishing fundamental value through switching costs lacks a singular approach, leading to inconclusive findings. We propose a robust approach to infer bubbles in the EU ETS. Empirical findings do not support the presence of a bubble in the third or fourth trading period.

JEL Code: C12 • G14 • Q01

1 Introduction

The theoretical articulation of a trading system as a measure to address market failure by utilizing transferable allowances was originally introduced by Coase (1960). To internalize the negative externality of climate change, the European Union (EU) introduced the European Emissions Trading System (EU ETS) in 2005 as a key climate protection instrument. Alongside other climate policy measures, this cap-and-trade system was initially intended to help reduce greenhouse gas emissions in the EU by at least 40% by 2030 compared to 1990 levels.

Overall, the EU ETS covers around 40% of total greenhouse gas emissions within the European Union. This makes the EU ETS the most comprehensive emissions trading system in the world. The participating states issue emission allowances partly free of charge, partly through auctions. One allowance permits the emission of one ton of CO_2 equivalents. Annually, firms subject to reporting obligations are required to submit an emissions report for the previous year and they are obligated to prove ownership of the corresponding number of allowances by the compliance date. Market participants have the option of banking allowances, given that the certificates maintain their validity not only within the compliance period but also extending into a subsequent trading period and beyond. Further, the right to freely trade these emission allowances establishes market prices for greenhouse gas emissions on the spot and futures market.

The total amount of greenhouse gas emissions per trading period that may be emitted by the approximately 13,500 production facilities subject to emissions trading in the 27 EU member states, Norway, Iceland and Liechtenstein is determined by a cap. In the first two trading periods (2005-2007 and 2008-2012), there was a massive oversupply of emission rights that were allocated largely free of charge. The resulting market prices were judged by the Organisation for Economic Co-operation and Development (OECD) to be too low to meet the political target in terms of emission reductions within the EU (see OECD, 2018). On the contrary, Bayer and Aklin (2020) empirically demonstrate that, despite low prices, the EU ETS effectively contributed to a significant reduction in emissions from 2008 to 2016.

To reinforce the effectiveness of the EU ETS to limit CO_2 emissions, with a price at around three euros per metric ton of CO_2 equivalents at the start of the third trading period in 2013, EU policymakers initiated a number of reforms: (i) Since the third trading period (2013-2020), a larger share of allowances has been auctioned to market participants, rather

than allocated freely as in the second trading period; (ii) during the first and second trading periods, there were national caps – with the third trading period, a uniform cap was set in the EU ETS; (iii) the EU adopted measures to reduce the amount of (surplus) allowances. The focus here is on the Market Stability Reserve (MSR), which gradually reduces the surplus in emissions trading and transfers it to a reserve from 2019 on.

Insert Figure 1 here.

Since 2018, there have been rapid price increases for the market price of emission allowances (see Figure 1). According to a 2019 survey by the Leibniz Centre for European Economic Research (see ZEW, 2019), 34% of market participants see the expected shortage of allowances due to the MSR as the main driver of the price increase, another 16% attribute it to the expectation of other tighter regulations, and 14% assume that speculation is behind the sharp price increases. With respect to the academic literature, there are several studies addressing excessive speculation and bubbles in the EU ETS. See, for most recent contributions, Jeszke and Lizak (2021), Wei, Li, and Wang (2022) and Quemin and Pahle (2023).

If the price hikes are indeed caused by a rational bubble, there would be uncertainty about the sustainability of the price increase since 2018 and whether a market correction should be anticipated in the future. In this case, the incentive created by the EU ETS for cost-effective emission reductions risks becoming ineffective. However, a massive drop in prices has not been observed since 2018 – on the contrary, prices have continued to rise with the fourth trading period (see Figure 1). Pahle, Günther, Osorio, and Quemin (2023) provide an analysis on various scenarios and developments related to the *endgame* anticipating a decade of critical changes in the EU ETS. In April 2023, the European Parliament adopted a new round of EU ETS reforms aligned with the *Fit For 55* package. These reforms include (i) a reduction in freely issued allowances and a stricter cap, with the *Linear Reduction Factor* for new allowances increasing from 2.2% per year to 4.4% starting in 2028 and (ii) two one-off reductions of allowances, known as *Rebasing*, are scheduled for 2024 and 2026. With the supply of new allowances expected to reach zero by 2040, these changes introduce substantial uncertainty into the market's long-term price dynamics and coincident with further price increases. Hence, the price of allowances might reflect market participants' expectations about the scarcity of allowances rather than the current switching costs, including the associated uncertainty. In this context, the primary objective of this paper is to offer an empirical analysis to determine whether the price increases over the third and fourth trading period can genuinely be attributed to a rational bubble.

On the one hand, the empirical evidence for a rational bubble in the EU ETS could be attributed to the existence of a rational bubble in the EU ETS or to the misspecification of the empirical proxy for the fundamental. Under the conditions that fuel-switching, i.e., investing in transitioning the production process from environmentally detrimental energy sources to environmentally friendly alternatives, is a perfect substitute for buying emission permits, producers will shift their production from cheaper but environmentally harmful energy sources to more expensive but cleaner alternatives. This transition will continue as long as the cost of reducing CO_2 emissions is lower than the price of allowances. In a state of market equilibrium without a rational bubble, the price in the EU ETS will align with the marginal abatement costs, see Montgomery (1972), Rubin (1996) and Kling and Rubin (1997) for deterministic equilibrium models. This forms the rationale for the folk principle considering switching costs as the fundamental in the EU ETS.

On the other hand, the interpretation of rational bubble tests based on switching costs assumes that the purchase of emission allowances is a perfect substitute for abatement solutions and this does not hold if market actors make decisions under uncertainty, e.g., uncertainty about allowance price determinants, market demand for products and services provided by CO_2 emitting firms or policy certainty, see Zhao (2003), Chesney and Taschini (2012) and Taschini (2021), or if transaction costs, e.g., informational and contractual costs, have an impact, see Baudry, Faure, and Quemin (2021). Further, deterministic equilibrium models assume that polluting firms comply with the regulation while stochastic equilibrium models take the non-compliant event directly into account, see Seifert, Uhrig-Homburg, and Wagner (2008), Carmona, Fehr, and Hinz (2009), Carmona, Fehr, Hinz, and Porchet (2010), Carmona and Hinz (2011), Chesney and Taschini (2012) and Hitzemann and Uhrig-Homburg (2018) for stochastic equilibrium models.[1]

We study the empirical implications of pricing equations for testing efficiency in an Emissions Trading Systems (ETS) on a solid foundation of rigorous economic theory. More specifically, we analyze the empirical implications of market equilibria, i.e., in the absence and presence of a rational bubble, within an ETS:

(i) Pricing with Switching Costs: Given that the EU ETS market price aligns with marginal abatement costs, see Carmona, Fehr, and Hinz (2009), we establish a pricing equation which implies a testable theoretical co-integration (co-explosiveness) vector. This

[1] See Chapter 7 in Chesney, Gheyssens, and Taschini (2013) for a comprehensive overview on deterministic and stochastic models for emission price dynamics.

vector should be evident in market equilibrium during non-explosive (explosive) episodes when no rational bubble is present.

(ii) Pricing with Market Expectations: For cases where the EU ETS market price deviates from marginal abatement costs, we examine the empirical implications of pricing equations based on market expectations, as discussed by Chesney and Taschini (2012) and Hitzemann and Uhrig-Homburg (2018). We differentiate between scenarios where banking is feasible or not within the trading system.

Given the option for market actors to bank certificates in the EU ETS, we propose a testing procedure that is based on the predictive regressions outlined by Fama (1984). This is referred to hereafter as the Fama Predictive Regression (FPR). We follow Pavlidis, Paya, and Peel (2017, 2018) using an endogenous instrumental variable based method (IVX), see Phillips and Magdalinos (2009), Kostakis, Magdalinos, and Stamatogiannis (2015) and Yang, Long, Peng, and Cai (2020), to estimate the FPR. Nevertheless, unlike the methodology proposed in Pavlidis, Paya, and Peel (2017) where a non-zero risk premium is restricted from being a component of the futures price, our method permits its inclusion.

Considering that purchasers (sellers) of certificates can hedge against anticipated price increases (decreases) on the futures market, it stands to reason that hedging pressure will arise, particularly in the event of strong price dynamics (see, among others, Bessembinder, 1992; Bessembinder and Chan, 1992; De Roon, Nijman, and Veld, 2000; Dewally, Ederington, and Fernando, 2013, for empirical evidence supporting the *Hedging Pressure Hypothesis* on futures markets). Notably, our approach is innovative in that it remains agnostic concerning the true fundamental and trend behavior of the risk premium. Thus, the risk premium can be explosive, which might be a phenomenon of economic relevance given rapidly growing price expectations. Therefore, this paper contributes also to the literature on testing against rational bubbles (see, among others, Phillips and Yu, 2011; Phillips, Shi, and Yu, 2015a,b; Harvey, Leybourne, Sollis, and Taylor, 2016; Pavlidis, Paya, and Peel, 2017, 2018).

Moreover, to examine whether the third trading phase (2013-2020) and the fourth trading phase (2021-ongoing) of the EU ETS have been free of rational bubbles (so far), we contribute with the following exercises to the empirical literature on carbon trading:

(i) We first investigate whether the EU ETS contains explosive episodes during the third and fourth trading period, which is a necessary condition for a rational bubble in

the EU ETS during this period. At this juncture, it seems acceptable to make a slight anticipation: We find pronounced explosiveness in EU ETS prices since 2018.

(ii) We estimate the predictive regression proposed by Fama (1984) employing the IVX technique by Kostakis, Magdalinos, and Stamatogiannis (2015) and using the IVX-AR approach by Yang, Long, Peng, and Cai (2020). This allows us to test against a rational bubble in the EU ETS in the presence of an (explosively) trending risk premium.

(iii) To either validate or challenge the outcomes of the FPR approach, we employ both the test by Phillips, Shi, and Yu (2015a,b) on the differential between future spot rates and futures rates and the test by Evripidou, Harvey, Leybourne, and Sollis (2022) on the future spot rates and futures rates, aiming to investigate the potential absence of a rational bubble in the EU ETS.

The paper is organized as follows: The following section elaborates on pricing equations in the EU ETS based on switching costs and based on market expectations. Section 3 proposes the econometric testing procedure and presents the results of a comprehensive Monte Carlo analysis. Section 4 describes the data and unveils the empirical findings of the paper. The concluding section, as outlined in Section 5, wraps up the discussion and delves into policy implications and potential directions for future research.

2 Pricing Equations for Emission Trading Systems

This section presents two fundamentally different approaches to price allowances in emissions trading systems: One is based on switching costs and the other on market expectations. The first approach relies on the implicit assumption that emission allowances are perfect substitutes for any technological abatement solution. Under this assumption, the ETS price should be determined by switching costs towards more CO_2-efficient energy sources (see Montgomery, 1972; Rubin, 1996; Kling and Rubin, 1997; Carmona, Fehr, and Hinz, 2009).

However, if market participants act under uncertainty and/or are faced with transaction costs, the assumption that allowances and fuel-switching are perfect substitutes is violated. Considering that investments in fuel-switching technologies often come with high costs, long-term durability, and irreversible investment requirements, they are typically not viewed as a perfect substitute to emission permits (see Chesney and Taschini, 2012; Taschini, 2021). Hence, the current spot price might reflect the expectation of scarcity of future emission

allowances rather than current switching costs. Therefore, we study in the following empirical implications of pricing equations based on expectations.

2.1 Pricing with Switching Costs

A rational bubble can be characterized as a situation where the price of an asset becomes disconnected from its underlying fundamental value. Within a rational expectations framework, rational bubbles emerge solely from the expectations of market actors regarding future price increases (see Flood and Hodrick, 1990). Since rational price expectations are positive, the price of the asset surges beyond its intrinsic value during a rational bubble (see Tirole, 1985; Diba and Grossman, 1988a,b).

We denote the price in the ETS as P_t, viz.

$$P_t = U_t + B_t \qquad \text{with} \qquad t = 1, 2, \ldots, T \tag{1}$$

where $U_t \geq 0$ is the fundamental value and $B_t \geq 0$ is the bubble component. The decomposition is orthogonal and hence, U_t and B_t are uncorrelated components of P_t. Blanchard (1979) suggests to model the bubble component as

$$B_t = \begin{cases} \frac{1+\rho}{\pi} \times B_{t-1} + \epsilon_t & \text{with probability } \pi, \\ \epsilon_t & \text{with probability } 1-\pi, \end{cases} \tag{2}$$

where $\rho > 0$ denotes the risk-free rate and ϵ_t is an independent and identically distributed (i.i.d.) random variable with zero mean and variance σ_ϵ^2, i.e., $\epsilon_t \sim \text{i.i.d.}\left(0, \sigma_\epsilon^2\right)$. We relax the i.i.d. assumption to allow for a general linear process, e.g., a stationary and invertible AutoRegressive Moving Average (ARMA) process. The bubble survives with probability π in period t. In this case, the bubble expands at an increased rate of $(1+\rho)/\pi$ to compensate investors for the potential bubble collapse. The bubble bursts with probability $1-\pi$ to white noise ϵ_t. We denote the conditional expectation given the information set $\mathscr{F}_t$ available at time t by $\mathbb{E}_t := \mathbb{E}[\cdot \mid \mathscr{F}_t]$. Since the bubble is a sub-martingale process, i.e.,

$$\mathbb{E}_t[B_{t+1}] = (1+\rho)B_t, \tag{3}$$

the bubble component of the price process B_t is explosive and expecting that $B_{t+1} > B_t$ is rational, hence the term *rational bubble* (see Diba and Grossman, 1988a). These

characteristics are also fulfilled, for example, by the periodically collapsing bubble process according to Evans (1991).

A time series with no deterministic component is said to be integrated of order d, denoted as $\mathrm{I}(d)$, if differencing the series d times results in a time series that has a stationary and invertible ARMA representation (see Engle and Granger, 1987). No finite number of differencing of an explosive process has a stationary and invertible ARMA presentation, viz. an explosive process is $\mathrm{I}(\infty)$ and therefore, the bubble component is integrated of order infinity, i.e., $B_t \sim \mathrm{I}(\infty)$, see Diba and Grossman (1988a). We use the notion of integration and the $\mathrm{I}(d)$-notation in the following to analyze the empirical implications for the ETS price given the presence or absence of a rational bubble, respectively.

Next, we delve into modeling the fundamental U_t: Assuming that emission allowances can perfectly substitute fuel-switching – meaning a transition from cheap but polluting to expensive but clean energy sources – producers will adjust their production processes. This adjustment will occur as long as the marginal cost of avoiding CO_2 emissions does not surpass the price of allowances (see Montgomery, 1972; Rubin, 1996; Kling and Rubin, 1997). Hence, in market equilibrium and assuming the absence of a rational price bubble, the price within the ETS aligns with the switching costs towards CO_2-efficient energy sources. Building on Carmona, Fehr, and Hinz (2009), the switching costs in the EU ETS are given as

$$S_t = \frac{\eta_{\text{gas}} \times P_t^{(\text{gas})} - \eta_{\text{coal}} \times P_t^{(\text{coal})}}{E_{\text{coal}} - E_{\text{gas}}}, \tag{4}$$

with $P_t^{(\text{gas})}$ and $P_t^{(\text{coal})}$ as the price of natural gas and the price of coal at time t, respectively. Further, the constant average CO_2 emissions for gas are given by

$$E_{\text{gas}} = 0.202 \frac{\mathrm{t}_{\mathrm{CO}_2}}{\mathrm{MWh}_{\text{therm}}} \times \frac{1}{0.52} \frac{\mathrm{MWh}_{\text{therm}}}{\mathrm{MWh}_{\text{el}}} = 0.388 \frac{\mathrm{t}_{\mathrm{CO}_2}}{\mathrm{MWh}_{\text{el}}}$$

and for coal are given by

$$E_{\text{coal}} = 0.341 \frac{\mathrm{t}_{\mathrm{CO}_2}}{\mathrm{MWh}_{\text{therm}}} \times \frac{1}{0.38} \frac{\mathrm{MWh}_{\text{therm}}}{\mathrm{MWh}_{\text{el}}} = 0.897 \frac{\mathrm{t}_{\mathrm{CO}_2}}{\mathrm{MWh}_{\text{el}}}$$

expressed in terms of metric tons of carbon emissions (t_{CO_2}) per Megawatt-hour (MWh) of electricity (MWh_{el}). Further, MWh_{therm} denotes a MWh of thermal power. The corresponding heat input coefficient is for gas

$$\eta_{gas} = \frac{1}{0.52}\frac{MWh_{therm}}{MWh_{el}} = 1.92\frac{MWh_{therm}}{MWh_{el}}$$

and for coal

$$\eta_{coal} = \frac{1}{6.961}\frac{t_{coal}}{MWh_{therm}} \times \frac{1}{0.38}\frac{MWh_{therm}}{MWh_{el}} = 0.378\frac{t_{coal}}{MWh_{el}}$$

where t_{coal} denotes one metric tone of coal. The precise numeric coefficients are obtained from Carmona, Fehr, and Hinz (2009).

Hence, the empirical pricing equation of emission allowances with $B_t = 0$ based on switching costs as the fundamental value reads as

$$P_t = \frac{\eta_{gas}}{E_{coal} - E_{gas}} \times P_t^{(gas)} - \frac{\eta_{coal}}{E_{coal} - E_{gas}} \times P_t^{(coal)} + \varepsilon_t, \tag{5}$$

where $P_t^{(gas)}$ and $P_t^{(coal)}$ are time series that are assumed to be integrated of order one, respectively. Further, let ε_t be a zero-mean innovation term integrated of order zero, i.e., $\varepsilon_t \sim I(0)$. Thus, ε_t might follow a stationary and invertible ARMA process.

Time series are said to be co-integrated when they share a common stochastic trend, meaning that there is a linear combination of these time series with a lower degree of integration than the underlying variables. Under the above assumptions about the underlying time series, the switching costs and the spot prices in the ETS are co-integrated with vector

$$\left(1, \psi_{gas}, \psi_{coal}\right)' := \left(1, \frac{\eta_{gas}}{E_{coal} - E_{gas}}, -\frac{\eta_{coal}}{E_{coal} - E_{gas}}\right)', \tag{6}$$

since $P_t \sim I(1)$, $P_t^{(gas)} \sim I(1)$, $P_t^{(coal)} \sim I(1)$ and $P_t - \psi_{gas} \times P_t^{(gas)} - \psi_{coal} \times P_t^{(coal)} = \varepsilon_t \sim I(0)$. Note that the expression on the right-hand side of Equation (5) also has the potential to exhibit explosiveness. Specifically, gas prices, coal prices, or both may be explosive (integrated of order infinity). In such a scenario, the ETS spot price would demonstrate an explosively trending behavior and share this explosive trend with gas and/or coal prices. In other words, ETS spot prices would exhibit co-explosiveness with gas and coal spot prices,

e.g., $P_t \sim \mathrm{I}(\infty)$, $P_t^{(\mathrm{gas})} \sim \mathrm{I}(\infty)$, $P_t^{(\mathrm{coal})} \sim \mathrm{I}(1)$ and $P_t - \psi_{\mathrm{gas}} \times P_t^{(\mathrm{gas})} - \psi_{\mathrm{coal}} \times P_t^{(\mathrm{coal})} = \varepsilon_t \sim \mathrm{I}(0)$.[2]

Pricing Equation 1 *With a potentially non-zero bubble component, it follows that the spot price process in the emission trading system, if emission certificates and switching costs are perfect substitutes, is given by*

$$\underbrace{P_t}_{\mathrm{I}(1)/\mathrm{I}(\infty)} = \frac{\eta_{gas}}{E_{coal} - E_{gas}} \times \underbrace{P_t^{(gas)}}_{\mathrm{I}(1)/\mathrm{I}(\infty)} - \frac{\eta_{gas}}{E_{coal} - E_{gas}} \times \underbrace{P_t^{(coal)}}_{\mathrm{I}(1)/\mathrm{I}(\infty)} + \underbrace{B_t}_{\mathrm{I}(\infty)} + \underbrace{\varepsilon_t}_{\mathrm{I}(0)}.$$

It becomes evident that when $B_t > 0$, the price dynamics P_t must exhibit explosiveness, and when $B_t = 0$, the price dynamics could potentially be explosive, contingent upon an explosive coal or gas price. Therefore, the presence of explosiveness in the price P_t alone does not provide adequate grounds to ascertain the existence of a rational bubble. Yet, when $B_t = 0$, the differential between the price and the switching costs is integrated to an order of zero, i.e., $P_t - S_t = \varepsilon_t \sim \mathrm{I}(0)$, since P_t and S_t are co-integrated or co-explosive, respectively. In contrast, when $B_t > 0$, the differential exhibits explosiveness, viz. $P_t - S_t = B_t + \varepsilon_t \sim \mathrm{I}(\infty)$. To examine the presence of a rational bubble within the ETS, one approach is to employ a right-sided unit root test on the differential between the ETS price and the switching costs. Empirical evidence in favor of the alternative, i.e., that $P_t - S_t$ is explosive, could argue for the existence of a rational bubble. However, rejecting the null hypothesis could stem from a misspecification of the fundamental, leading to inconclusive outcomes. For example, Creti and Joëts (2017) determine the fundamental of the EU ETS as $0.520 \times P_t^{(\mathrm{gas})} + 0.632 \times P_t^{(\mathrm{oil})} + 0.514 \times S_t - 0.260 \times P_t^{(\mathrm{stock})}$ by principle component analysis, whereas $P_t^{(\mathrm{oil})}$ denotes the price for crude oil and $P_t^{(\mathrm{stock})}$ is the value of an appropriate stock market index at time t. Specifying the fundamental in this way is in marked contrast to the specification based solely on switching costs as in Equation (5), highlighting the different interpretations of the *true* underlying fundamental in the ETS and the possibility of misspecification.

Consequently, discovering a method to identify a rational bubble without the need to explicitly define a fundamental is essential, particularly in the context of an ETS. It becomes even more crucial considering an additional limitation of the switching costs approach, which assumes that investments in fuel-switching technologies and the acquisition of emission allowances are perfect substitutes. In situations where market participants are

[2]There is the possibility of co-integration or co-explosiveness between gas and coal prices. Nevertheless, since these instances are not pertinent to the subsequent analysis, they will not be elaborated upon here.

faced with transaction costs or if market actors anticipate alterations in future switching costs, varying penalties for non-compliance, or a potential adjustment in the quantity of certificates available, the perfect substitutes assumption might be violated and the validity of Pricing Equation 1 would be compromised (see Zhao, 2003; Chesney and Taschini, 2012; Taschini, 2021; Baudry, Faure, and Quemin, 2021). Especially due to dynamic political measures to reduce CO_2 emissions, the assumption that market actors decide under certainty appears unrealistic (see Pahle, Günther, Osorio, and Quemin, 2023). The next section provides an approach which does not require the assumption that fuel-switching and buying certificates are perfect substitutes.[3]

2.2 Pricing with Market Expectations

Chesney and Taschini (2012) formulate an equilibrium model for the price dynamics of emission allowances, incorporating the presence of asymmetric information. As a result, the equilibrium price of allowances is determined by the market actor's expectations of either scarcity or surplus of allowances in the market. Expanding upon their results and on the findings by Hitzemann and Uhrig-Homburg (2018), our goal within this section is to introduce a pricing equation based on market expectation to analyse rational bubbles in ETS. We begin with an approach that assumes the absence of banking possibilities. Following this, we delve into a perspective that accommodates banking, which aligns more realistically with the context of the EU ETS.

Banking in the context of this paper means that market actors are allowed to use certificates beyond the current compliance date $\mathscr{T}$ and they exercise this option when they anticipate an increase in allowance prices. In order to fix ideas, consider the forward contract written at time t with delivery date $\mathscr{T}$: The bubble component is eliminated from the forward price if the delivery date equals the compliance date $\mathscr{T}$, as the forward contract can only be used for compliance and not longer for speculation. However, if it is possible to bank, speculation can continue beyond $\mathscr{T}$, and the bubble component does not necessarily disappear from the price expectations. However, as pointed out by Pavlidis, Paya, and Peel (2017, 2018), under rational bubbles, the weighting of the bubble part in the price

[3] Given that the assumptions of an empirical study relying on the switching costs approach seem overly restrictive, we will refrain from analyzing co-integration or co-explosiveness in the following empirical analysis. However, note that there are several studies that analyze a potential co-integration equilibrium between switching costs and emission prices (see Creti, Jouvet, and Mignon, 2012; Koch, Fuss, Grosjean, and Edenhofer, 2014; Rickels, Görlich, and Peterson, 2015). Further, see Hintermann, Peterson, and Rickels (2016) for a comprehensive review on the empirical literature about allowance price dynamics during phase II.

expectations differs from the weighting of the bubble component in the actual spot price. As the fundamental components are weighted equally in the equations for prices and price expectations, explosiveness in the differential between price expectations and the actual prices indicates conclusively a rational bubble.

2.2.1 Trading without Banking Opportunities

If the ETS does not allow for banking, the value of an allowance at time t for a regulated firm i, denoted as $U_{i,t}$, can be thought of as the expected discounted probability-weighted penalty $\varpi_{\mathscr{T}}$, which firm $i = 1, 2, \ldots, I$ would have to pay if it fails to provide enough certificates by the compliance date $\mathscr{T}$ (see Carmona, Fehr, and Hinz, 2009; Chesney and Taschini, 2012; Hitzemann and Uhrig-Homburg, 2018). Hence, we receive the fundamental in the ETS from the perspective of firm i as

$$U_{i,t} = (1+\rho)^{-(\mathscr{T}-t)} \times \mathbb{E}_{i,t}\left[\varpi_{\mathscr{T}} \times \left(1-\mathscr{P}_{i,\mathscr{T}}\right)\right], \tag{7}$$

whereas $t \in (0, \mathscr{T}]$, $\mathscr{P}_{i,\mathscr{T}}$ is the probability that firm i fails to comply with the regulations at time $\mathscr{T}$ and $\mathbb{E}_{i,t} := \mathbb{E}\left[\cdot \mid \mathscr{F}_{i,t}\right]$ denotes conditional expectation given the information set $\mathscr{F}_{i,t}$ available for firm i at time t. Next, consider the price of a forward contract, denoted by $F_{i,\mathscr{T},t}$, written by firm i at time t with delivery date $\mathscr{T}$, i.e., the price of a forward contract that guarantees delivery of allowances at compliance date to firm i. Given that market actors are risk-neutral, the price of this forward contract at time t corresponds to the expected probability-weighted penalty, viz.

$$F_{i,\mathscr{T},t} = \mathbb{E}_{i,t}\left[\varpi_{\mathscr{T}} \times \left(1-\mathscr{P}_{i,\mathscr{T}}\right)\right], \tag{8}$$

as any speculation on elevated prices beyond time $\mathscr{T}$ is irrational from the perspective of firm i without banking. Hence, the speculative element, i.e., the influence of the bubble component within this forward contract must approach zero as the delivery date approaches compliance date $\mathscr{T}$. Chesney and Taschini (2012) show in a multi-firm trading setup and under asymmetric information about emission levels of individual firms that the discounted equilibrium fundamental process is a martingale and free of arbitrage opportunities. Correspondingly, Hitzemann and Uhrig-Homburg (2018) receive a cost-of-carry model similar to

$$U_t = (1+\rho)^{-(\mathscr{T}-t)} \times F_{\mathscr{T},t} + \nu_t. \tag{9}$$

It is important to mention that in this context, $\nu_t \sim \mathrm{I}(0)$ incorporates the convenience yield, as discussed in detail by Trück and Weron (2016).

Pricing Equation 2 *The assumption of risk-neutral agents ensures that $F_{\mathscr{T},t}$ is equivalent to market expectations. Hence, in the absence of the ability to bank certificates, the spot price in the ETS is determined for risk-neutral agents as*

$$P_t = (1+\rho)^{-(\mathscr{T}-t)} \times F_{\mathscr{T},t} + B_t + \nu_t.$$

Given that $\nu_t \sim \mathrm{I}(0)$, for $B_t = 0$, the differential

$$D_{\mathscr{T},t} := P_t - (1+\rho)^{-(\mathscr{T}-t)} \times F_{\mathscr{T},t}, \tag{10}$$

is integrated of order zero, i.e.,

$$\underbrace{D_{\mathscr{T},t}}_{\mathrm{I}(0)} = \underbrace{\nu_t}_{\mathrm{I}(0)} \tag{11}$$

and for $B_t > 0$, the differential is integrated of order infinity, i.e.,

$$\underbrace{D_{\mathscr{T},t}}_{\mathrm{I}(\infty)} = \underbrace{B_t}_{\mathrm{I}(\infty)} + \underbrace{\nu_t}_{\mathrm{I}(0)}. \tag{12}$$

Hence, applying a right-sided unit root test to $D_{\mathscr{T},t}$ would allow to draw consistent inference about a rational bubble. Moving forward, we examine a trading scheme that permits banking and is thus more in alignment with the EU ETS.

2.2.2 Trading with Banking Opportunities

Taking into account the opportunity for banking among market participants beyond period $\mathscr{T}$, the forward (futures) price could contain a bubble component. Hitzemann and Uhrig-Homburg (2018) propose a stochastic equilibrium model that takes banking directly into account. The authors show that the equilibrium permit price without a rational bubble, i.e., the fundamental value, is given by

$$U_t = \sum_{p=k}^{N_{\mathscr{T}}} (1+\rho)^{-(\mathscr{T}_p - t)} \times \mathbb{E}_t\left[U_{\mathscr{T}_p}\right] \tag{13}$$

allowing for permit banking, whereas $t \in (\mathscr{T}_{k-1}, \mathscr{T}_k]$ and $N_{\mathscr{T}}$ denotes the number of compliance periods of the ETS.

Pricing Equation 3 *If banking is allowed in the emission trading system, the spot price in the ETS is determined as*

$$P_t = \sum_{p=k}^{N_{\mathscr{T}}} (1+\rho)^{-(\mathscr{T}_p - t)} \times \mathbb{E}_t\left[U_{\mathscr{T}_p}\right] + B_t.$$

Hence, the price with a bubble component at time $t+n$ is given by

$$\begin{aligned} P_{t+n} &= U_{t+n} + B_{t+n} = \sum_{p=k}^{N_{\mathscr{T}}} \left((1+\rho)^{-(\mathscr{T}_p - t - n)} \times \mathbb{E}_{t+n}\left[U_{\mathscr{T}_p}\right] \right) + B_{t+n} \\ &= \sum_{p=k}^{N_{\mathscr{T}}} \left((1+\rho)^{-(\mathscr{T}_p - t - n)} \times \mathbb{E}_{t+n}\left[U_{\mathscr{T}_p}\right] \right) + \left(\frac{1+\rho}{\pi}\right)^n B_t + \epsilon_{t+n} \end{aligned} \tag{14}$$

with $(t+n) \in (\mathscr{T}_{k-1}, \mathscr{T}_k]$. For the price expectations at time t about time $t+n$, we receive

$$\begin{aligned} \mathbb{E}_t\left[P_{t+n}\right] &= \sum_{p=k}^{N_{\mathscr{T}}} \left((1+\rho)^{-(\mathscr{T}_p - t - n)} \times \mathbb{E}_t\left[U_{\mathscr{T}_p}\right] \right) + \mathbb{E}_t\left[B_{t+n}\right] \\ &= \sum_{p=k}^{N_{\mathscr{T}}} \left((1+\rho)^{-(\mathscr{T}_p - t - n)} \times \mathbb{E}_t\left[U_{\mathscr{T}_p}\right] \right) + (1+\rho)^n \times B_t \end{aligned} \tag{15}$$

with $(t+n) \in (\mathscr{T}_{k-1}, \mathscr{T}_k]$. The differential between actual and expected ETS prices is given by

$$D_{t+n} := P_{t+n} - \mathbb{E}_t\left[P_{t+n}\right] = \vartheta_{t+n} + (1+\rho)^n \left(\frac{1}{\pi^n} - 1\right) \times B_t + \epsilon_{t+n}, \tag{16}$$

whereas the prediction error of the fundamental component reads as

$$\vartheta_{t+n} = \sum_{p=k}^{N_{\mathscr{T}}} \left((1+\rho)^{-(\mathscr{T}_p - t - n)} \times \mathbb{E}_{t+n}\left[U_{\mathscr{T}_p}\right] \right) - \sum_{p=k}^{N_{\mathscr{T}}} \left((1+\rho)^{-(\mathscr{T}_p - t - n)} \times \mathbb{E}_t\left[U_{\mathscr{T}_p}\right] \right) \tag{17}$$

and ϵ_{t+n} is the prediction error for the bubble component. Note that ϑ_{t+n} when $B_t = 0$ and $\vartheta_{t+n} + \epsilon_{t+n}$ when $B_t > 0$ correspond to the prediction which minimizes the mean-squared prediction error (MSPE). This is because, by definition, conditional expectation minimizes the MSPE under quadratic loss, see Granger (1969) and Baumeister (2023).

With $\vartheta_{t+n} \sim \mathrm{I}(0)$ and $\vartheta_{t+n} + \epsilon_{t+n} \sim \mathrm{I}(0)$, respectively, we receive for $B_t = 0$,

$$\underbrace{D_{t+n}}_{\mathrm{I}(0)} = \underbrace{\vartheta_{t+n}}_{\mathrm{I}(0)} \tag{18}$$

and for $B_t > 0$, we obtain

$$\underbrace{D_{t+n}}_{\mathrm{I}(\infty)} = \underbrace{\vartheta_{t+n}}_{\mathrm{I}(0)} + (1+\rho)^n \left(\frac{1}{\pi^n} - 1 \right) \times \underbrace{B_t}_{\mathrm{I}(\infty)} + \underbrace{\epsilon_{t+n}}_{\mathrm{I}(0)}. \tag{19}$$

Hence, the differential D_{t+n} does not depend on the market fundamental, see Pavlidis, Paya, and Peel (2017, 2018). This implies that the explosive dynamics of the differential between spot (see Equation 14) and expected spot prices (see Equation 15) are due solely to the presence of a rational bubble.

Hence, one might consider employing a right-sided unit root test to assess explosiveness in D_{t+n}. However, it is crucial to acknowledge that $\mathbb{E}_t[P_{t+n}]$ is not observable. To tackle the challenges stemming from this lack of observability, we introduce a novel approach in the following sections.

3 Testing against Rational Bubbles in the Presence of a Risk Premium

The predominant empirical method for evaluating rational bubbles has been introduced by Phillips and Yu (2011) and Phillips, Shi, and Yu (2015a,b). Their proposed approach involves testing against explosive behavior in the differential between fundamental and price series. Moreover, these scholars present robust right-sided unit root tests, aiming to overcome concerns raised by Evans (1991) regarding the limited power of standard unit root and co-integration tests in detecting periodically collapsing bubbles. One limitation of employing explosiveness testing in the differential between fundamental and price series to assess rational bubbles is its dependence on a proxy for the fundamental process. Although this concern might be manageable in the realm of stocks, where the dividend process is observable and can act as a substitute for the fundamental, the preceding chapter underscored the challenges associated with defining the fundamental in the context of an ETS.

Pavlidis, Paya, and Peel (2017, 2018) address this challenge by investigating market expectations instead of opting for a proxy for the fundamental. Consequently, Pavlidis, Paya, and Peel (2017) utilize the continuous futures price at time t with a delivery date of $t+n$, represented as $F_{n,t}$, as a proxy of market expectations. However, this approach comes with a limitation, as the risk premium, which accounts for the difference between the futures price and the market expectation, remains unobservable. Based on the current state of the literature, this necessitates a decision between making assumptions about the trending behavior of the risk premium or estimating the risk premium from the futures price series, as deliberated by Hamilton and Wu (2014). Subsequently, we investigate an approach that eliminates the need for both.[4]

[4]It is crucial to acknowledge that employing the Hamilton and Wu (2014) method for estimating the market expectations includes an inherent estimation error. This error extends to right-sided unit root tests employed for rational bubble inference, potentially resulting in significant size distortions. Hence, we abstain from estimating market expectations in the initial stage and subsequently employing these expectations for bubble testing in the second stage.

3.1 The Role of the Risk Premium

As stated previously in Section 2.2.2, Equation (16) predicts a stationary equilibrium between actual prices and price expectations in the absence of a rational bubble. Should the researcher opt for assuming a stationary risk premium, denoted as $RP_{n,t} \sim \mathrm{I}(0)$ where

$$RP_{n,t} := F_{n,t} - \mathbb{E}_t\left[P_{t+n}\right], \tag{20}$$

she can apply a stationarity test to $P_{t+n} - F_{n,t}$ to test against the presence of a rational bubble. However, rejecting the null hypothesis of stationarity of $P_{t+n} - F_{n,t}$ could arise from either a bubble price component or a non-stationary risk premium. Moreover, if the researcher is willing to assume an integrated risk premium of order one, i.e., $RP_{n,t} \sim \mathrm{I}(1)$, a right-sided unit root test might be employed. Rejecting the null hypothesis of no rational bubble in this scenario could be attributed to either a rational bubble or an explosive risk premium, denoted as $RP_{n,t} \sim \mathrm{I}(\infty)$.

Is an explosive risk premium a phenomenon that holds economic relevance? To answer this question, we define the risk premium as in Equation (20), a negative (positive) risk premium indicates *normal backwardation* (*normal contango*) in the futures market, i.e., $F_{n,t} < \mathbb{E}_t\left[P_{t+n}\right]$ $\left(F_{n,t} > \mathbb{E}_t\left[P_{t+n}\right]\right)$. Originally proposed by Keynes (1930) and Hicks (1939), the notion of normal backwardation posits that hedgers typically maintain short positions as an insurance against the market price risk. The *Insurance Hypothesis* implies that the futures price should be lower than the expected future spot price, acting as compensation to the speculator for furnishing insurance to the producer. More generally, the *Hedging Pressure Hypothesis* states that, in normal backwardation (normal contango), the risk premium is driven by sellers (buyers) engaged in future contracts to insure against anticipated price decreases (increases), see, among others, Bessembinder (1992), Bessembinder and Chan (1992), De Roon, Nijman, and Veld (2000), and Dewally, Ederington, and Fernando (2013) for empirical support in favor of the Hedging Pressure Hypothesis.

In the context of an ETS, firms regulated and holding surplus emission certificates may choose to sacrifice a premium to shift the price risk to the long position, viz. they are willing to receive the certainty equivalent $\mathbb{E}_t\left[\mathscr{U}\left(P_{t+n}\right)\right]$ whereas $\mathbb{E}_t\left[\mathscr{U}\left(P_{t+n}\right)\right] < \mathbb{E}_t\left[P_{t+n}\right]$. In this case $\mathscr{U}(\cdot)$ denotes the utility function of a representative agent holding the short position. Conversely, firms facing a shortage of certificates might be inclined to pay a premium to transfer the price risk to the short position, viz. these agents are willing to pay the certainty

equivalent $\mathbb{E}_t\left[\mathscr{U}\left(P_{t+n}\right)\right]$ whereas $\mathbb{E}_t\left[\mathscr{U}\left(P_{t+n}\right)\right] > \mathbb{E}_t\left[P_{t+n}\right]$. In this case $\mathscr{U}(\cdot)$ denotes the utility function of a representative agent holding the long position.

In both scenarios (normal contango or normal backwardation), the resulting time-varying risk premium depends on the spot price:

$$RP_{n,t} = \mathbb{E}_t\left[\mathscr{U}\left(P_{t+n}\right)\right] - \mathbb{E}_t\left[P_{t+n}\right] + \varphi_t. \tag{21}$$

Here, φ_t is a zero-mean $\mathrm{I}(0)$ innovation term whose variance is labeled as σ^2_{φ}. This implies that $\mathrm{Cov}\left(B_t, RP_{n,t}\right) \neq 0$ and $\mathrm{Cov}\left(U_t, RP_{n,t}\right) \neq 0$ might be pertinent, whereas $\mathrm{Cov}(\cdot,\cdot)$ denotes the population covariance. To illustrate the potential economic significance of a trending risk premium with utmost simplicity, we assume that $\mathscr{U}(\cdot)$ is linear, i.e.,

$$\mathbb{E}_t\left[\mathscr{U}\left(P_{t+n}\right)\right] = (1+\varrho)\,\mathbb{E}_t\left[P_{t+n}\right], \tag{22}$$

whereas ϱ denotes the risk aversion parameter with $-1 < \varrho < 0$ in a normal backwardation situation and $\varrho > 0$ in a normal contango situation. Hence, we receive the time-varying risk premium as

$$RP_{n,t} = \varrho \times \left((1+\rho)^n B_t + \theta^n U_t\right) + \varphi_t, \tag{23}$$

whereas $\mathrm{Cov}(U_t, B_t) = 0$ and the fundamental follows an autoregressive process, expressed as $U_t = \theta U_{t-1} + \vartheta_t$, where $\theta \geq 1$ represents the autoregressive coefficient. This formulation ensures co-explosiveness (co-integration) between the risk premium and the bubble (and the fundamental) component with the vector

$$\left(1, \psi_{n,B}, \psi_{n,U}\right)' := \left(1, \varrho\,(1+\rho)^n, \varrho\,\theta^n\right)'$$

such that $\mathrm{Cov}\left(B_t, RP_{n,t}\right) = \varrho\,(1+\rho)^n \mathrm{Var}(B_t)$ and $\mathrm{Cov}\left(U_t, RP_{n,t}\right) = \varrho\,\theta^n \mathrm{Var}(U_t)$. The potential co-explosiveness between bubble (fundamental) and risk premium, renders an explosive risk premium a phenomenon of economic relevance.

3.2 Fama Predictive Regressions

In this section, we showcase a method based on FPRs that is robust against the trending behavior of the risk premium. Specifically, the rejection rates of the newly suggested test statistic align with the nominal level under the null hypothesis of no rational bubble (size of the test). Additionally, our method exhibits decent power properties to infer rational bubbles under different conditions, such as a stationary risk premium, $RP_{n,t} \sim \mathrm{I}(0)$; an integrated risk premium of order one, $RP_{n,t} \sim \mathrm{I}(1)$; and an explosive risk premium, $RP_{n,t} \sim \mathrm{I}(\infty)$.

Fama (1984) splits the futures price at time t and delivery date $t+n$ into the expected price at time t with respect to time $t+n$ and a risk premium $RP_{n,t}$, i.e.,

$$F_{n,t} = \mathbb{E}_t\left[P_{t+n}\right] + RP_{n,t} \tag{24}$$

to receive the differential between the futures price and the current price, i.e.,

$$F_{n,t} - P_t = \mathbb{E}_t\left[P_{t+n}\right] - P_t + RP_{n,t}, \tag{25}$$

and to obtain the differential between the futures price and future spot price, i.e.,

$$F_{n,t} - P_{t+n} = \mathbb{E}_t\left[P_{t+n}\right] - P_{t+n} + RP_{n,t}. \tag{26}$$

Bearing this in mind, Fama (1984) considers the two regressions

$$\begin{aligned}
&\text{(FPR 1)} \qquad F_{n,t} - P_{t+n} &&= \mu_{1,n} + \beta_{1,n}\left(F_{n,t} - P_t\right) + e_{1,t+n},\\
&\text{(FPR 2)} \qquad P_{t+n} - P_t &&= \mu_{2,n} + \beta_{2,n}\left(F_{n,t} - P_t\right) + e_{2,t+n},
\end{aligned}$$

whereas $\mu_{1,n}$ and $\mu_{2,n}$ are constants, $\beta_{1,n}$ and $\beta_{2,n}$ are slope coefficients and $e_{1,t+n}$ and $e_{2,t+n}$ are disturbances with mean zero. Given that there is no rational bubble, we obtain from Equation (16), Equation (25) and Equation (26) the slope coefficient of FPR 1 as

$$\beta_{1,n} := \frac{\mathrm{Cov}\left(F_{n,t} - P_{t+n}, F_{n,t} - P_t\right)}{\mathrm{Var}\left(F_{n,t} - P_t\right)} = \frac{\mathrm{Cov}\left(-\vartheta_{t+n} + RP_{n,t}, \mathbb{E}_t\left[P_{t+n}\right] - P_t + RP_{n,t}\right)}{\mathrm{Var}\left(F_{n,t} - P_t\right)}, \tag{27}$$

whereas $\mathrm{Var}(\cdot)$ denotes the population variance. For $\mathrm{Cov}\left(\vartheta_{t+n}, RP_{n,t}\right) = 0$ and $\mathrm{Cov}\left(\vartheta_{t+n}, P_t\right) = 0$, we receive

$$\beta_{1,n} = \frac{\mathrm{Var}\left(RP_{n,t}\right) + \mathrm{Cov}\left(RP_{n,t}, \mathbb{E}_t\left[P_{t+n}\right] - P_t\right)}{\mathrm{Var}\left(RP_{n,t}\right) + \mathrm{Var}\left(\mathbb{E}_t\left[P_{t+n}\right] - P_t\right) + 2\,\mathrm{Cov}\left(RP_{n,t}, \mathbb{E}_t\left[P_{t+n}\right] - P_t\right)}. \tag{28}$$

For $\beta_{2,n}$, i.e., the slope coefficient of FPR 2, we obtain

$$\beta_{2,n} := \frac{\mathrm{Cov}\left(P_{t+n}-P_t, F_{n,t}-P_t\right)}{\mathrm{Var}\left(F_{n,t}-P_t\right)} = \frac{\mathrm{Cov}\left(\mathbb{E}_t\left[P_{t+n}\right]-P_t+\vartheta_{t+n}, \mathbb{E}_t\left[P_{t+n}\right]-P_t+RP_{n,t}\right)}{\mathrm{Var}\left(F_{n,t}-P_t\right)} \tag{29}$$

and with the above argument, i.e., $\mathrm{Cov}\left(\vartheta_{t+n}, RP_{n,t}\right) = 0$ and $\mathrm{Cov}\left(\vartheta_{t+n}, P_t\right) = 0$, we receive

$$\beta_{2,n} = \frac{\mathrm{Var}\left(\mathbb{E}_t\left[P_{t+n}\right]-P_t\right)+\mathrm{Cov}\left(RP_{n,t}, \mathbb{E}_t\left[P_{t+n}\right]-P_t\right)}{\mathrm{Var}\left(RP_{n,t}\right)+\mathrm{Var}\left(\mathbb{E}_t\left[P_{t+n}\right]-P_t\right)+2\,\mathrm{Cov}\left(RP_{n,t}, \mathbb{E}_t\left[P_{t+n}\right]-P_t\right)}. \tag{30}$$

Fama (1984) notes that both FPRs convey identical information, resulting in $\beta_{1,n}+\beta_{2,n} = 1$, $\mu_{1,n}+\mu_{2,n} = 0$ and the disturbances sum up to zero for each time period t.

3.2.1 Slope Coefficients $\beta_{1,n}$ and $\beta_{2,n}$ under an Ongoing Rational Bubble

Next, we analyze $\beta_{1,n}$ and $\beta_{2,n}$ under an ongoing rational bubble. We assume that the fundamental follows a mildly explosive process, viz. $U_t = \theta U_{t-1}+\vartheta_t$ where $\theta = 1+c\times T^{-\alpha}$ and $c > 0$, $\alpha \in (0,1)$ such that $\theta = 1$ as $T \to \infty$, as discussed in Phillips and Magdalinos (2007). For a data generating processes (DGP) characterized by mild explosiveness, the autoregressive coefficient surpasses unity, with the extent of its deviation from unity diminishing as the sample size increases. This process has been demonstrated to effectively capture the features of moderately explosive behavior observed in various economic and financial time series. Since future innovations are uncorrelated with fundamental and bubble component, i.e., $\mathrm{Cov}\left(\vartheta_{t+n}, U_t\right) = \mathrm{Cov}\left(\epsilon_{t+n}, B_t\right) = 0$, we receive

$$\beta_{1,n} = \frac{\mathrm{Var}\left(RP_{n,t}\right)-\gamma_{1,n}\mathrm{Var}\left(B_t\right)+\gamma_{2,n}\,\mathrm{Cov}\left(B_t, RP_{n,t}\right)}{\mathrm{Var}\left(RP_{n,t}\right)+\gamma_n^2\mathrm{Var}\left(B_t\right)+2\gamma_n\,\mathrm{Cov}\left(B_t, RP_{n,t}\right)} \qquad \text{as} \qquad T \to \infty, \tag{31}$$

whereas $\gamma_n := (1+\rho)^n - 1$,

$$\gamma_{1,n} := (1+\rho)^n\left(\frac{1}{\pi^n}-1\right)\left((1+\rho)^n-1\right) \qquad \text{and} \qquad \gamma_{2,n} := 2(1+\rho)^n - \left(\frac{1+\rho}{\pi}\right)^n - 1$$

and

$$\beta_{2,n} = \frac{\gamma_{3,n}\mathrm{Var}\left(B_t\right)+\gamma_{4,n}\,\mathrm{Cov}\left(B_t, RP_{n,t}\right)}{\mathrm{Var}\left(RP_{n,t}\right)+\gamma_n^2\mathrm{Var}\left(B_t\right)+2\gamma_n\,\mathrm{Cov}\left(B_t, RP_{n,t}\right)} \qquad \text{as} \qquad T \to \infty, \tag{32}$$

with

$$\gamma_{3,n} := \left(\left(\frac{1+\rho}{\pi}\right)^n - 1\right)((1+\rho)^n - 1) \qquad \text{and} \qquad \gamma_{4,n} := \left(\frac{1+\rho}{\pi}\right)^n - 1.$$

Note that $\gamma_n^2 = -\gamma_{1,n} + \gamma_{3,n}$ and $2\gamma_n = \gamma_{2,n} + \gamma_{4,n}$ leading to the conclusion that $\beta_{1,n} + \beta_{2,n} = 1$, see Fama (1984). A detailed derivation can be found in Appendix A.

As a result, when $B_t = 0$, i.e., $\text{Var}(B_t) = 0$ and $\text{Cov}\left(B_t, RP_{n,t}\right) = 0$, we obtain $\beta_{1,n} = 1$ and $\beta_{2,n} = 0$. In the scenario where $B_t > 0$, we distinguish between the case that $\text{Cov}\left(B_t, RP_{n,t}\right) = 0$ and that $\text{Cov}\left(B_t, RP_{n,t}\right) \neq 0$. For $\text{Cov}\left(B_t, RP_{n,t}\right) = 0$, we receive

$$\begin{aligned} \beta_{1,n} &= \frac{\text{Var}\left(RP_{n,t}\right) - \gamma_{1,n}\text{Var}(B_t)}{\text{Var}\left(RP_{n,t}\right) + \gamma_n^2 \text{Var}(B_t)} \leq 1 \quad \text{and} \\ \beta_{2,n} &= \frac{\gamma_{3,n}\text{Var}(B_t)}{\text{Var}\left(RP_{n,t}\right) + \gamma_n^2 \text{Var}(B_t)} \geq 0 \quad \text{as} \quad T \to \infty \end{aligned} \tag{33}$$

with $\dfrac{\partial \beta_{1,n}}{\partial \text{Var}(B_t)} < 0, \quad \dfrac{\partial \beta_{1,n}}{\partial \text{Var}\left(RP_{n,t}\right)} > 0, \quad \dfrac{\partial \beta_{2,n}}{\partial \text{Var}(B_t)} > 0, \quad \dfrac{\partial \beta_{2,n}}{\partial \text{Var}\left(RP_{n,t}\right)} < 0$

for $\rho > 0$, $0 < \pi \leq 1$ and $n \in \mathbb{Z}$ with $n \geq 1$. This implies that $\beta_{1,n}$ decreases monotonically below one and that $\beta_{2,n}$ increases monotonically above zero as $\text{Var}(B_t)$ increases, in particular $\beta_{1,n} \to \left((1+\rho)^n - \left(\frac{1+\rho}{\pi}\right)^n\right)/\gamma_n$ and $\beta_{2,n} \to \left(\left(\frac{1+\rho}{\pi}\right)^n - 1\right)/\gamma_n$ as $\text{Var}(B_t) \to \infty$, respectively.

Moreover, we explore the scenario where $\text{Cov}\left(B_t, RP_{n,t}\right) \neq 0$. Based on the notion of a futures market in contango, i.e., $\psi_{n,B} > 0$ and $\psi_{n,U} > 0$, or backwardation i.e., $\psi_{n,B} < 0$ and $\psi_{n,U} < 0$, we obtain $\text{Var}\left(RP_{n,t}\right) = \psi_{n,B}^2 \times \text{Var}(B_t) + \psi_{n,U}^2 \times \text{Var}(U_t) + \sigma_\varphi^2$ and $\text{Cov}\left(B_t, RP_{n,t}\right) = \psi_{n,B} \times \text{Var}(B_t)$. This yields

$$\begin{aligned} \beta_{1,n} &= \frac{\sigma_\varphi^2 + \left(\left(\psi_{n,B} + \gamma_n\right)^2 - \gamma_{3,n} - \psi_{n,B}\gamma_{4,n}\right)\text{Var}(B_t) + \psi_{n,U}^2 \text{Var}(U_t)}{\sigma_\varphi^2 + \left(\psi_{n,B} + \gamma_n\right)^2 \text{Var}(B_t) + \psi_{n,U}^2 \text{Var}(U_t)} \leq 1 \quad \text{and} \\ \beta_{2,n} &= \frac{\left(\gamma_{3,n} + \psi_{n,B}\gamma_{4,n}\right)\text{Var}(B_t)}{\sigma_\varphi^2 + \left(\psi_{n,B} + \gamma_n\right)^2 \text{Var}(B_t) + \psi_{n,U}^2 \text{Var}(U_t)} \geq 0 \quad \text{as} \quad T \to \infty, \end{aligned} \tag{34}$$

with $\dfrac{\partial \beta_{1,n}}{\partial \text{Var}(B_t)} < 0, \quad \dfrac{\partial \beta_{1,n}}{\partial \text{Var}(U_t)} > 0, \quad \dfrac{\partial \beta_{2,n}}{\partial \text{Var}(B_t)} > 0, \quad \dfrac{\partial \beta_{2,n}}{\partial \text{Var}(U_t)} < 0$

for $\rho > 0, 0 < \pi \leq 1, n \in \mathbb{Z}$ with $n \geq 1$ and $\psi_{n,B} + \gamma_n > 0$. Hence, we need to impose the assumption that $\psi_{n,B} + \gamma_n > 0$ if $\psi_{n,B} < 0$ to ensure that $\beta_{1,n}$ decreases monotonously below one and that $\beta_{2,n}$ increases monotonously above zero as $\mathrm{Var}(B_t)$ increases. In particular $\beta_{1,n} \to \left(\psi_{n,B} + (1+\rho)^n - \left(\frac{1+\rho}{\pi}\right)^n\right) / \left(\psi_{n,B} + \gamma_n\right)$ and $\beta_{2,n} \to \left(\left(\frac{1+\rho}{\pi}\right)^n - 1\right) / \left(\psi_{n,B} + \gamma_n\right)$ as $\mathrm{Var}(B_t) \to \infty$, respectively.[5]

3.2.2 Drawing Inference on $\beta_{1,n}$ and $\beta_{2,n}$

We are interested in testing

$$\begin{aligned} &\mathscr{H}_0 : \beta_{1,n} = 1 \quad \text{(no rational bubble)} \quad \text{vs.} \quad \mathscr{H}_A : \beta_{1,n} < 1 \quad \text{(rational bubble)}, \\ &\mathscr{H}_0 : \beta_{2,n} = 0 \quad \text{(no rational bubble)} \quad \text{vs.} \quad \mathscr{H}_A : \beta_{2,n} > 0 \quad \text{(rational bubble)} \end{aligned}$$

using the conventional t-test based on the OLS method without the need to specify the fundamental or impose assumptions on the trending behavior of the risk premium. However, with a significant level of persistence in the explanatory variable, the conventional t-test results derived from the OLS method lose their validity. Stambaugh (1999) has demonstrated convincingly that this issue becomes more pronounced when the disturbances in the predictive regression are strongly correlated with the regressor's innovations.

Kostakis, Magdalinos, and Stamatogiannis (2015) present the IVX procedure that strengthens the robustness of inference concerning the degree of persistence of the explanatory variable, encompassing mildly explosive behavior. More explicitly, by replacing the regressor, denoted in the following by $x_t := F_{n,t} - P_t$, with an instrument z_t – characterized by a controllable level of persistence – results in a robust inference procedure that addresses the impacts of non-stationarity. We denote the regressand by y_t, i.e., $y_t := F_{n,t} - P_{t+n}$ for FPR 1 and $y_t := P_{t+n} - P_t$ for FPR 2. The IVX estimator of the slope coefficient of the FPR is given by

$$\widehat{\beta}^{IVX} = \frac{\sum_{t=1}^{T} z_t \widetilde{y}_t}{\sum_{t=1}^{T} z_t \widetilde{x}_t}, \tag{35}$$

whereas $\widetilde{x}_t$ and $\widetilde{y}_t$ denote demeaned counterparts of x_t and y_t, respectively. Kostakis, Magdalinos, and Stamatogiannis (2015) demonstrate the convergence of $\widehat{\beta}^{IVX}$ to a mixed Gaussian limiting distribution, a result that remains valid irrespective of the level of persistence exhibited by the regressors in the model. As a result, this feature facilitates the development of a Wald-type statistic, denoted as W_β, which converges to a standard χ^2-

[5] Note that, since the IVX approach (to estimate the slope coefficients) employs demeaned variables, we do not derive $\mu_{1,n}$ and $\mu_{2,n}$.

distribution. We make use of the IVX estimator for FPR 2 and we study the performance of the corresponding Wald statistic, see Kostakis, Magdalinos, and Stamatogiannis (2015), for testing $\beta_{2,n} = 0$ against $\beta_{2,n} \neq 0$ in the following section (the rational for opting to test against $\beta_{2,n} \neq 0$ instead of testing against $\beta_{2,n} > 0$ is provided below).

3.3 Monte Carlo Simulation

We analyse the finite-sample properties of the FPR approach with $n = 1$ applied to test against rational bubbles. For additional simulation studies encompassing a prediction period exceeding one, i.e., $n \in \{2, 3, 4\}$, we refer the reader to Appendix C. We specifically examine cases where the sample size takes on values from the set $T \in \{150, 300\}$, aligning with our subsequent empirical analysis.[6]

3.3.1 Monte Carlo Simulation: Size

We start with the size, i.e., we consider the rejection rates of a Wald statistic, as proposed by Kostakis, Magdalinos, and Stamatogiannis (2015), for the hypothesis that $\beta_{2,n} = 0$ against $\beta_{2,n} \neq 0$ when $P_t = U_t$. Under the null hypothesis, the fundamental is generated as

$$U_t = \theta U_{t-1} + \vartheta_t \qquad \text{whereas} \qquad \theta = 1 + c \times T^{-\alpha} \qquad \text{and} \qquad \vartheta_t \sim \text{i.i.d.} N(0, 1)$$

with $c = 0.1$, $\alpha \in \{0.7, 0.75, 0.8, 0.85\}$ and $U_0 = 100$, i.e., the fundamental is explosive and therefore the price series fulfills the necessary condition for a rational bubble. The risk premium is simulated by two distinct DGPs under the null hypothesis, denoted as RP 1 and RP 2 respectively:

$$\begin{aligned}
&\text{(RP 1)} \quad RP_{n,t} = \lambda RP_{n,t-1} + \varphi_t \quad \text{where} \quad \varphi_t \sim \text{i.i.d.} N(0, 1) \quad \text{and} \quad \lambda \in \{0, 0.5, 1, 1.01\}, \\
&\text{(RP 2)} \quad RP_{n,t} = \varrho \theta U_t + \varphi_t \quad \text{where} \quad \varphi_t \sim \text{i.i.d.} N(0, 1) \quad \text{and} \quad \varrho \in \{-0.01, +0.01\}.
\end{aligned}$$

Hence, under specification RP 1, we consider a risk premium which is stationary, i.e., $\lambda \in \{0, 0.5\}$, integrated of order one, i.e., $\lambda = 1$, and explosive, i.e., $\lambda = 1.01$. Further,

[6] The `exuber` package in R was employed to simulate bubble processes and compute the SADF, BSADF, and GSADF test statistic along with their corresponding critical values, as detailed in (see Vasilopoulos, Pavlidis, and Martínez-García, 2022). It is worth noting that FPR 1 and FPR 2 contain identical information. Therefore, evaluating the performance of either regression is sufficient for testing rational bubbles. In this study, we opt for FPR 2 to facilitate the use of the `ivx` R-package (see Vasilopoulos and Pavlidis, 2020) for testing $\beta_{2,n} = 0$ versus $\beta_{2,n} \neq 0$.

under specification RP 2, we examine a risk premium that shares an explosive trend with the fundamental. This enables an examination of $\text{Cov}\left(U_t, RP_{n,t}\right) \neq 0$. Specifically, we obtain $\text{Cov}\left(U_t, RP_{n,t}\right) = \varrho\theta\,\text{Var}\left(U_t\right)$, where $\varrho > 0$ ($\varrho < 0$) ensures that $\text{Cov}\left(U_t, RP_{n,t}\right) > 0$ $\left(\text{Cov}\left(U_t, RP_{n,t}\right) < 0\right)$. Furthermore, it is important to observe that the risk premium specification RP 1, where $\lambda \in \{0, 0.5\}$, implies that the representative agent involved in the futures market is characterized as risk-neutral. In contrast, specifications RP 2 (and RP 3 below) are in line with either normal contango or normal backwardation. Conversely, RP 1 with $\lambda \in \{1, 1.01\}$ corresponds to a scenario where agents are not risk-neutral, however, the risk premium is influenced by factors other than market prices.

As a natural competitor we apply the KPSS test to $P_{t+1} - F_{1,t}$, see Kwiatkowski, Phillips, Schmidt, and Shin (1992), as Equation (16) predicts a stationary differential between actual prices and price expectations in the absence of a rational bubble. Table 1 outlines the results of a Monte Carlo simulation with 10,000 repetitions and a nominal size of 5%. The left panel contains the results for the FPR method and the right panel shows the results of the KPSS test with $\lfloor 4(T/100)^{0.25} \rfloor = 4$ lags (whereas $\lfloor \cdot \rfloor$ indicates the floor function).

Insert Table 1 here.

We observe that the trend behavior of $RP_{n,t}$ does not carry significance for the rejection rates in testing $\beta_{2,n} = 0$ (or $\beta_{1,n} = 1$). Although the variance of $RP_{n,t}$ increases with a higher degree of integration, resulting in a loss of power, as illustrated below, the test's size remains uninfluenced by the trend in $RP_{n,t}$. This is due to the fact that, regardless of the risk premium's trend behavior, the numerator in Equation (31) (Equation 32) consistently maintains a value of zero (one) under the null hypothesis. In particular, as anticipated, the KPSS test maintains its nominal size when the risk premium is stationary. However, this ceases to be the case when the risk premium is integrated of order one or explosive. Hence, the KPSS test is unreliable in these cases.

3.3.2 Monte Carlo Simulation: Estimation

Next, we study the performance of the IVX approach to estimate $\beta_{2,n}$ given that the price process is generated by $P_t = U_t + B_t$ with $B_t > 0$. Throughout the analysis, we assume that the fundamental is generated by a random walk, i.e., $U_t = U_{t-1} + \vartheta_t$ with $\vartheta_t \sim \text{i.i.d.}N(0, 1)$. In examining size, it is crucial for either the fundamental and/or the risk premium to exhibit explosiveness; otherwise, the empirical analysis of a rational bubble is not justified, as the

necessary condition for a rational bubble remains unmet. However, in the scenario where the price exhibits a non-zero bubble component, i.e., under the alternative hypothesis, the fundamental may manifest as a random walk. While there is the potential for the fundamental to exhibit explosiveness also under the alternative hypothesis, it is cautious to presume a random walk for the fundamental to rule out a positive effect on power due to a non-zero covariance between explosive fundamental and risk premium. Under the alternative, the risk premium is generated by RP 1 or by

$$\text{(RP 3)} \qquad RP_{n,t} = \varrho \times (1+\rho) B_t + \varrho \times \theta U_t + \varphi_t,$$

where $\varphi_t \sim$ i.i.d. $N(0,1)$ and $\varrho \in \{-0.01, +0.01\}$.

We examine the estimates of $\beta_{2,n}$ based on Blanchard's DGP as described in Equation (2) under the assumption that the bubble does not burst. We do this to demonstrate that, fundamentally, our results are comparable to those presented by Pavlidis, Paya, and Peel (2017). The bubble price component is generated by

$$\text{(B 1)} \quad B_t = \frac{1+\rho}{\pi} B_{t-1} + \epsilon_t \qquad \text{whereas} \qquad \epsilon_t \sim \text{i.i.d.} N(0, 0.3),$$

$B_0 = 20$ and $T = 150$. Given that the bubble is continuing and that the risk premium is generated by RP 3, we receive the theoretical slope coefficient as

$$\beta_{2,n} = \frac{(\varrho(1+\rho)+\rho)(1-\pi+\rho)\operatorname{Var}(B_t)}{\pi\left(\sigma_\varphi^2 + (\varrho(1+\rho)+\rho)^2 \operatorname{Var}(B_t) + \varrho\theta \operatorname{Var}(U_t)\right)} \quad \text{as} \quad T \to \infty \tag{36}$$

whereas $\operatorname{Var}(U_t) = t\sigma_\varphi^2$ (since the fundamental is generated by a random walk) and $\operatorname{Var}(B_t) = \left(\left(\frac{1+\rho}{\pi}\right)^{2t} - 1\right) / \left(\left(\frac{1+\rho}{\pi}\right)^2 - 1\right)\sigma_\epsilon^2$, see Fuller (2009).

Insert Table 2 here.

Table 2 outlines the theoretical value of $\beta_{2,n}$, the arithmetic mean and the standard deviation, denoted by Mean and SD, respectively, of the IVX estimates for $\beta_{2,n}$ with 10,000 simulated price paths of a non-collapsing bubble according to DGP B 1 with $\rho = 0.1$ and $\pi \in \{0.3, 0.5, 0.7, 0.9\}$ following the simulation study by Pavlidis, Paya, and Peel (2017). It is noteworthy that, given the specified price process, there should be an approximate difference of -1 between the slope coefficient outlined in Table 1 in Pavlidis, Paya, and Peel (2017) and the slope coefficient for FPR 2 in Table 2 for $\lambda = \varrho = 0$ (we refrain from

exploring additional values for λ since the variance of the risk premium is dominated by the variance of the bubble, rendering the variance of the risk premium negligible). The relatively low standard deviations observed in all cases are consistent with the findings in Pavlidis, Paya, and Peel (2017).

Further, we consider the estimation of the slope coefficient for FPR 2 given that the bubble component of $P_t = U_t + B_t$ is generated by Blanchard (1979) and by Evans (1991) whereas the bubble collapses potentially. For both DGPs, the sample size is chosen to be T from the set $\{150, 300\}$ and the fundamental is generated by $U_t = U_{t-1} + \vartheta_t$ with $\vartheta_t \sim$ i.i.d.$N(0,1)$. Blanchard's DGP is generated by

$$\text{(B 2)} \qquad B_t = \begin{cases} \frac{1+0.1}{\pi} \times B_{t-1} + \epsilon_t & \text{with probability } \pi, \\ \epsilon_t & \text{with probability } 1-\pi, \end{cases}$$

whereas $\epsilon_t \sim$ i.i.d.$N\left(0, 0.3^2\right)$, $B_0 = 20$ and $\pi \in \{0.3, 0.5, 0.7, 0.9\}$. For Evans' DGP the following specification applies

$$\text{(B 3)} \qquad B_{t+1} = \begin{cases} (1+\rho) B_t \xi_{t+1}, & \text{if} \quad B_t \leq 1, \\ \left[0.5 + \frac{1}{\pi}(1+\rho)\varsigma_{t+1}\left(B_t - \frac{0.5}{(1+\rho)}\right)\right]\xi_{t+1}, & \text{if} \quad B_t > 1, \end{cases}$$

whereas ξ_t follows a lognormal distribution, viz. $\xi_t = \exp\left(\kappa_t - 0.05^2/2\right)$ with $\kappa_t \sim$ i.i.d.$N\left(0, 0.05^2\right)$, and ς_t is a Bernoulli process, taking the value of 1 with probability π and the value of 0 with probability $1-\pi$ whereas $\pi \in \{0.3, 0.5, 0.7, 0.9\}$. Note that this process fulfills also rational expectations. We adhere to Evans (1991) and to Pavlidis, Paya, and Peel (2017) and scale bubbles generated from DGP B3 by a factor of 20 in the subsequent simulation study.

Insert Table 3 here.

Table 3 presents the outcomes from 10,000 Monte Carlo replications and the risk premium is generated by DGP RP 1 (upper panel) and DGP RP 3 (lower panel). When dealing with the (periodically) collapsing bubbles, it becomes evident that the mean of the IVX estimates for $\beta_{2,n}$ consistently takes on negative values. This observation can be attributed to an autoregressive coefficient within the stationary region, specifically below one, of the price process during the collapse of the rational bubble. We could leverage this observation, akin to the methodology introduced by Pavlidis, Paya, and Peel (2017), by utilizing the change in sign of the slope coefficient in a rolling-window approach to

timestamp the bubble phase. It is pertinent to note that while Pavlidis, Paya, and Peel (2017) thoroughly examined the rolling-window approach, we refrain from further discussion on this topic here, emphasizing that the same rolling-window methodology is applicable to FPR 2. However, our subsequent attention is directed toward a full-sample approach. Hence, we conduct the test against $\beta_{2,n} \neq 0$ instead of $\beta_{2,n} > 0$ because a collapsing bubble would imply $\beta_{2,n} < 0$, while an ongoing bubble suggests $\beta_{2,n} > 0$. Consequently, to account for both surviving and bursting bubbles, we specify the alternative as $\beta_{2,n} \neq 0$ rather than $\beta_{2,n} > 0$.

3.3.3 Monte Carlo Simulation: Power

The absolute value of the mean of the IVX estimates for $\beta_{2,n}$ diminishes with the rise in the value of λ. As the latter has a negative effect on power, we analyse the rejection rates of the Wald statistic, as outlined by Kostakis, Magdalinos, and Stamatogiannis (2015), applied to the FPR approach under identical specifications as for the simulation with regard to the estimation of the slope coefficient. As a competitor we employ the Generalized Supremum Augmented Dickey Fuller test (GSADF) which tests under the null hypothesis that the differential $P_{t+1} - F_{1,t}$ has a unit root against the temporary explosive alternative. This approach is the natural choice under the assumption that the risk premium is $\mathrm{I}(1)$. Further, it is known that full-sample stationarity and unit roots tests have little power to indicate bubbles which arise and collapse. In contrast, the GSADF test is recognized for its good power properties in the presence of (periodically) collapsing bubbles.

Insert Table 4 here.

Table 4 offers a synopsis of the rejection rates for the Wald statistic (left panel) and the GSADF test (right panel). This summary is based on a nominal size of 5% and 10,000 replications, considering the Blanchard bubble and the risk premium is generated by DGP RP 1 (upper panel) and by DGP RP 3 (lower panel). Likewise, Table 5 presents the rejection rates of the Wald statistic and the GSADF approach under identical conditions, maintaining a nominal size of 5% and 10,000 replications, with a focus on the Evans bubble.

Insert Table 5 here.

In the realm of assessing rational bubbles in conjunction with a risk premium integrated of order one or explosive, the FPR approach stands out for maintaining its nominal size. This

is a crucial consideration, as inaccurately identifying a bubble could lead to misguided policy recommendations and result in significant adverse economic and political consequences. However, it is crucial to recognize that this robustness comes with trade-offs, resulting in a decrease in the power of the FPR approach as the persistence of the risk premium increases. This increase in persistence leads to an elevated variance of the risk premium. Consequently, it holds that as $\text{Var}\left(RP_{n,t}\right) \to \infty$, we obtain $\beta_{1,n} \to 1$ and $\beta_{2,n} \to 0$, resulting in a loss of power of the FPR approach, all else being equal. A similar outcome arises when there is correlation between the risk premium and the bubble and fundamental component, respectively, coupled with an increasing variance of the fundamental since as $\text{Var}\left(U_t\right) \to \infty$, we obtain also $\beta_{1,n} \to 1$ and $\beta_{2,n} \to 0$. In contrast, the power of the GSADF test remains unaffected by the trending behavior of the risk premium in all considered cases.

Moreover, the power of the FPR approach capitalizes on an increasing (decreasing) covariance between the risk premium and the bubble component, all else being equal. On the contrary, the GSADF test's power remains unaffected if the covariance varies. Thus, the FPR approach effectively utilizes the information of the non-zero covariance in contrast to the GSADF test. As a result, our overall findings indicate that, although the FPR approach may not definitively surpass the GSADF approach in inferring a rational bubble in every considered case, it exhibits superior performance in the majority of scenarios (especially under a stationary risk premium, normal backwardation or normal contango).

4 Data and Empirical Results

Prior to delving into the empirical findings, we begin this section by introducing the data employed in our empirical analysis. Next, we investigate whether market prices and futures prices show explosive behavior using the Supremum Augmented Dickey Fuller test (SADF) and the GSADF test (see Phillips, Shi, and Yu, 2015a,b). Subsequently, we turn to the core of our analysis, and we test the pair of hypotheses

$$\mathscr{H}_0 : \beta_{2,n} = 0 \quad \text{(no rational bubble)} \qquad \text{vs.} \qquad \mathscr{H}_A : \beta_{2,n} \neq 0 \quad \text{(rational bubble)}$$

for the third trading phase (2013-2020) and the fourth trading phase (2021-ongoing) of the EU ETS. We employ the IVX approach by Kostakis, Magdalinos, and Stamatogiannis (2015) and the IVX-AR method by Yang, Long, Peng, and Cai (2020) to tackle potential distortions in size in the testing procedure proposed by Kostakis, Magdalinos, and Stamatogiannis

(2015) when serial correlation and heteroskedasticity are present in the error term of the predictive regression. To emphasize or contest the results of the FPR approach, we apply also the competitors from the Monte Carlo simulation above: The GSADF approach (and the SADF approach) by Phillips, Shi, and Yu (2015a,b) applied to the difference between future spot rates and futures rates, and the method by Evripidou, Harvey, Leybourne, and Sollis (2022) examining co-explosiveness between future spot rates and futures rates.

4.1 Data

We utilize weekly price data from the Bloomberg database spanning from January 4, 2013, to October 11, 2023, encompassing a total of $T = 563$ observations. The Bloomberg abbreviation for the spot price is `ICEDEU3 Index`. All fundamental contracts were actively traded and monitored on the Intercontinental Currency Exchange (ICE). Based on these contracts, our analysis focuses on generic continuous futures prices with a delivery date of one, two, three and four months, respectively. Since we consider weekly data, we receive $n \in \{4, 8, 12, 16\}$, i.e., delivery in 4, 8, 12 and 16 weeks. Contracts with $n > 4$ are excluded due to a lack of liquidity.

4.2 Is there an Explosive Episode in EU ETS Spot and Futures Rates?

We start our empirical exercise with testing against explosive episodes in the EU ETS price and futures price series over the full sample from 2013 to 2023. Explosiveness in spot prices is a necessary but, as described above, not a sufficient condition for a rational bubble. Nevertheless, the timing of when the spot price becomes explosive holds significance for subsample analysis, such as predictive regression and co-explosiveness analysis, in the subsequent sections.

We employ the SADF and GSADF test on the spot and futures price series in its original levels, and we find evidence for explosive behavior at the 5% significance level indicated by superscript r, as reported in Table 6.

Insert Table 6 here.

The critical values for the SADF and GSADF test are determined by wild bootstrapping with 999 repetitions accounting for multiplicity and heteroskedasticity (see Phillips and

Shi, 2020). Further, the test uses $T = 563$ observations and a minimum window size of $r_0 := \lfloor 0.01 + 1.8\sqrt{T} \rfloor = 42$ observations, following the rule proposed by Phillips, Shi, and Yu (2015a,b). Furthermore, as highlighted by Vasilopoulos, Pavlidis, and Martínez-García (2022), simulations provide evidence suggesting the effective performance of the SADF and GSADF tests when a limited fixed number of lags is employed. In contrast, utilizing information criteria for lag selection may lead to notable distortions in size. As a result, we adopt the approach proposed by Pavlidis, Yusupova, Paya, Peel, Martínez-García, Mack, and Grossman (2016), employing two variations of a fixed number of lags. Specifically, we integrate one and four lags within the augmented Dickey-Fuller regression.

Subsequently, our next objective is to date-stamp the beginning and the end of the explosive periods. Hence, we use the Backward Supremum Augemented Dickey Fuller (BSADF) sequence with bootstrapped critical values (see Phillips, Shi, and Yu, 2015a,b; Phillips and Shi, 2020). Overall, our findings for the spot and futures price series reveal (i) consistent indications of explosiveness across all series, and (ii) a notably similar timing pattern of the explosive phases in spot and futures prices during the third and fourth trading phase. The results are summarized by Figure 2 and Figure 3, indicating episodes of explosive behavior during the end of the third and during the fourth trading period.

Insert Figures 2 and 3 here.

4.3 Is there a Rational Bubble in the EU ETS?

As the date stamping reveals periods of explosive price behavior in the third trading period from 2018 to its closure 2022 and at the commencement of the fourth trading period 2021 up to 2023, our analysis below concentrates on two specific approaches. First, we conduct a full-sample analysis by employing the Fama predictive regression covering the period from January 2018 to October 2023, i.e., $T = 302$. Second, we perform a subsample analysis, examining the third and fourth trading periods separately, creating a subset from January 2018 to December 2020, i.e., $T = 156$, and another from January 2021 to October 2023, i.e., $T = 146$.

We estimate the predictive regression by the IVX method and we test $\beta_{2,n} = 0$ against $\beta_{2,n} \neq 0$ using the Wald statistic, see Kostakis, Magdalinos, and Stamatogiannis (2015). Moreover, we employ the IVX-AR procedure as outlined in Yang, Long, Peng, and Cai (2020) to account for potential distortions in size in the testing procedure proposed by Kostakis,

Magdalinos, and Stamatogiannis (2015) when serial correlation and heteroskedasticity are present in the error term of the predictive regression.

Insert Tables 7 and 8 here.

The outcomes are detailed in Table 7 for the full-sample analysis, i.e., we consider the third (since 2018) and fourth trading periods together, and in Table 8 for the sub-sample analysis, i.e., we consider the third (since 2018) and fourth trading period separately. The value of the Wald test statistic introduced by Kostakis, Magdalinos, and Stamatogiannis (2015) is denoted by W_β, $\widetilde{W}_\beta$ is the value of the Wald test statistic introduced by Yang, Long, Peng, and Cai (2020) and $|t_\beta|$ denotes the absolute value of the t-statistic in the OLS case for comparison.

Further, W_{AR} denotes the Wald statistic for the joint hypothesis that all included lags in the error term of FPR 2 are equal to zero, see Yang, Long, Peng, and Cai (2020) for details. The corresponding $p-$values are outlined in parentheses. Note that we determine the lag length to account for autocorrelation in the error term of FPR 2 by the Bayesian Information Criterion (BIC). The results corresponding to W_{AR} in Table 7 and Table 8 highlight the need to account for serial correlation in the error term.

Therefore, we concentrate on the outcomes associated with the IVX-AR method. Employing this approach, we fail to reject the null hypothesis that $\beta_{2,n} = 0$ in favor of the alternative $\beta_{2,n} \neq 0$ in all considered cases. This contradicts the presence of a collapsing bubble ($\beta_{2,n} < 0$) or an ongoing bubble ($\beta_{2,n} > 0$). These results are consistent across both the full-sample analysis and the sub-sample analyzes.

4.4 Further Empirical Evidence

In order to either confirm or contest the findings of the Fama predictive regression approach, we utilize both the test conducted by Phillips, Shi, and Yu (2015a,b) on the differential between future spot rates and futures rates and the test by Evripidou, Harvey, Leybourne, and Sollis (2022) on the future spot rates and futures rates.

4.4.1 Testing against Explosiveness in the Differential between Future Spot Rates and Futures Rates

Given that the risk premium is integrated of order d_{RP}, i.e., $RP_{n,t} \sim \mathrm{I}(d_{RP})$, whereas $d_{RP} \in [0,1]$, it stands to reason to consider the empirical model

$$P_{t+n} - F_{n,t} = \mu_D + \theta_D \left(P_{t-1+n} - F_{n,t-1}\right) + u_{t+n}, \tag{37}$$

whereas u_{t+n} is a martingale difference sequence, μ_D is the drift component and θ_D is the autoregressive parameter, and to test

$$\mathscr{H}_0 : \theta_D \leq 1 \quad \text{(no rational bubble)} \qquad \text{vs.} \qquad \mathscr{H}_A : \theta_D > 1 \quad \text{(rational bubble)}.$$

Similar to the scenario where spot and futures rates are considered, critical values for the SADF and GSADF tests are derived through wild bootstrapping with 999 repetitions, taking into account multiplicity and heteroskedasticity (see Phillips and Shi, 2020). The test is implemented with $T = 563$ observations and a minimum window size of 42, adhering to the guideline proposed by Phillips, Shi, and Yu (2015a,b).

Insert Table 9 here.

Table 9 presents the outcomes of the test by Phillips, Shi, and Yu (2015a,b) with one and four lags, applied to the differential between future spot rates and futures rates with $n \in \{4, 8, 12, 16\}$ weeks. Our findings reveal no evidence of explosiveness in the differential between future spot rates and futures rates, indicating a lack of support for the presence of a rational bubble or an explosive risk premium.

4.4.2 Testing against Co-Explosiveness between Future Spot Rates and Futures Rates

Ultimately, we examine the co-explosiveness of the EU ETS price and its expectations. To establish the absence of a rational bubble, a sufficient condition is that futures prices, i.e., $F_{n,t}$, and spot prices, i.e., P_{t+n}, share a common (explosive) trend. Therefore, we employ the approach introduced by Evripidou, Harvey, Leybourne, and Sollis (2022). Hence, we test

$$\mathscr{H}_0 : \beta_F > 0,\ \beta_Z = 0 \text{ (no rational bubble) vs. } \mathscr{H}_A : \beta_F = 0,\ \beta_Z > 0 \text{ (rational bubble)}$$

with

$$P_{t+n} = \mu_P + \beta_F F_{n,t} + \beta_Z Z_{t+n} + \omega_{t+n} \tag{38}$$

whereas μ_P is a constant, the unobserved variable Z_{t+n} contains the bubble component $B_{t+n} > 0$ and ω_{t+n} equals ϑ_{t+n} for $B_t = 0$ or aggregates ϵ_{t+n} and ϑ_{t+n} for $B_t > 0$. The spot price and futures prices (including the stationary risk premium) exhibit co-explosiveness according to the null hypothesis. Under the alternative, the spot price and the expectations differ by an explosive component, i.e., the explosive risk premium or the explosive bubble component. Hence, if the null hypothesis is not rejected, we can infer the absence of a bubble component. However, rejecting it does not definitively establish the presence of a rational bubble.

The approach by Evripidou, Harvey, Leybourne, and Sollis (2022) utilizes a KPSS-type test (see Kwiatkowski, Phillips, Schmidt, and Shin, 1992) on $\hat{\omega}_{t+n}$ whereas $\hat{\omega}_{t+n} = P_{t+n} - \hat{\mu}_P - \hat{\beta}_F F_{n,t}$ and $\hat{\mu}_P$ and $\hat{\beta}_F$ are OLS estimates. This approach accounts for heteroskedasticity by a wild bootstrap procedure (see Liu, 1988; Mammen, 1993). Further, note that we use the approach by Newey and West (1994) with a quadratic spectral kernel with automated lag selection to estimate the long-run variance employed in the test statistic.

Insert Table 10 here.

Table 10 presents the test statistics and their corresponding 5% critical values, determined through wild bootstrap, for the entire sample period from January 2018 to October 2023. The testing for co-explosiveness between futures and spot rates leads to rejecting the null hypothesis for all examined values of n, suggesting the presence of either an explosive bubble component or another non-stationary component, e.g., a non-stationary risk premium.

Insert Table 11 here.

However, Table 11 displays the outcomes from the sub-sample analysis covering January 2018 to December 2021 (left panel) and January 2022 to October 2023 (right panel). When distinguishing between the third and fourth trading periods, we do not find evidence to reject the null hypothesis, indicating the absence of a rational bubble during either period. Consequently, the results across the entire sample could be influenced by a structural break (e.g., a mean shift) in the risk premium leading a rejecting of the null hypothesis that future spot and futures rates are co-explosive. Thus, the co-explosiveness test results align with those from the FPR approach.

5 Conclusion, Discussion and Future Research

The significance of addressing climate change emphasizes the utmost importance of emission trading systems operating optimally. Therefore, it is crucial to leverage the insights acquired from previous trading phases for shaping the design of future emission trading systems and for implementation of best possible regulations. As emission trading schemes play a central role in climate policy, understanding their market dynamics and potential for improvement is of paramount importance.

This paper adds to the existing body of research on climate finance, with a specific focus on carbon trading, see Hong, Karolyi, and Scheinkman (2020). The empirical investigation, in particular, aims to enhance our understanding of whether the notable rise in EU ETS prices since 2018 can be linked to a rational bubble. However, the analysis reveals no evidence of a rational bubble being the driving force behind the surge in allowance prices in 2018. Instead, it implies that the surge in EU ETS prices could be attributed to the expectation of impending scarcity, stemming from significant policy changes affecting emission caps. This is supported by the parallel (explosive) trend behavior observed in both future spot rates and futures rates.

Although we refrain from asserting the superiority of a Pigouvian tax or a trading system in mitigating carbon emissions, a significant drawback of a trading system would be the potential for excessive speculation resulting in a (rational) bubble. We alleviate concerns regarding speculation that triggered a rational bubble in previous trading phases. Therefore, in our perspective, there is no necessity for policy intervention to prevent potential rational bubbles in the EU ETS architecture, given the analysis of historical data at our disposal.

Our research, in our view, opens up various possibilities for future research. First, we have demonstrated that Fama Predictive Regressions can be used to test against rational bubbles also in the presence of a time-trending risk premium. Hence, FPRs can be employed across various asset classes where futures prices are observable, without the necessity of assuming the trend behavior of the risk premium or establishing a fundamental. This includes bonds, commodities, currencies, stocks but also certificates of other emission trading systems.

Second, Quemin and Pahle (2023) established a diagnostic toolkit to evaluate the extent and consequences of speculation for an emission trading system, subsequently applying it to the EU ETS. Nonetheless, a heightened level of speculation alone does not inherently imply market inefficiency. Therefore, it is reasonable to employ FPRs within a rolling window approach to provide a real-time perspective to indicate inefficiency of emission trading systems.

Third, analyzing the price expectations of market participants in the ETS can serve not only for testing against a rational bubble but also for evaluating the effectiveness of the ETS in reducing carbon emissions, especially in comparison to a tax, see Martinsson, Strömberg, Sajtos, and Thomann (2023). Further, it would be intriguing to explore whether and when investments in research and development rise in anticipation of higher future prices in the ETS, see Brown, Martinsson, and Thomann (2022).

References

Baudry, M., A. Faure, and S. Quemin. 2021. Emissions trading with transaction costs. *Journal of Environmental Economics and Management* 108:102468–.

Baumeister, C. 2023. Measuring market expectations. *Handbook of Economic Expectations* 413–41.

Bayer, P., and M. Aklin. 2020. The European Union emissions trading system reduced CO2 emissions despite low prices. *Proceedings of the National Academy of Sciences* 117:8804–12.

Bessembinder, H. 1992. Systematic risk, hedging pressure, and risk premiums in futures markets. *The Review of Financial Studies* 5:637–67.

Bessembinder, H., and K. Chan. 1992. Time-varying risk premia and forecastable returns in futures markets. *Journal of Financial Economics* 32:169–93.

Blanchard, O. J. 1979. Speculative bubbles, crashes and rational expectations. *Economics Letters* 3:387–9.

Brown, J. R., G. Martinsson, and C. Thomann. 2022. Can environmental policy encourage technical change? Emissions taxes and R&D investment in polluting firms. *The Review of Financial Studies* 35:4518–60.

Carmona, R., M. Fehr, and J. Hinz. 2009. Optimal stochastic control and carbon price formation. *SIAM Journal on Control and Optimization* 48:2168–90.

Carmona, R., M. Fehr, J. Hinz, and A. Porchet. 2010. Market design for emission trading schemes. *SIAM Review* 52:403–52.

Carmona, R., and J. Hinz. 2011. Risk-neutral models for emission allowance prices and option valuation. *Management Science* 57:1453–68.

Chesney, M., J. Gheyssens, and L. Taschini. 2013. *Environmental finance and investments*. Springer.

Chesney, M., and L. Taschini. 2012. The endogenous price dynamics of emission allowances and an application to CO2 option pricing. *Applied Mathematical Finance* 19:447–75.

Coase, R. H. 1960. The problem of social cost. *The Journal of Law and Economics* 3:1–44.

Creti, A., and M. Joëts. 2017. Multiple bubbles in the European Union Emission Trading Scheme. *Energy Policy* 107:119–30.

Creti, A., P.-A. Jouvet, and V. Mignon. 2012. Carbon price drivers: Phase I versus Phase II equilibrium? *Energy Economics* 34:327–34.

De Roon, F. A., T. E. Nijman, and C. Veld. 2000. Hedging pressure effects in futures markets. *The Journal of Finance* 55:1437–56.

Dewally, M., L. H. Ederington, and C. S. Fernando. 2013. Determinants of trader profits in commodity futures markets. *The Review of Financial Studies* 26:2648–83.

Diba, B. T., and H. I. Grossman. 1988a. Explosive rational bubbles in stock prices? *The American Economic Review* 78:520–30.

———. 1988b. Rational inflationary bubbles. *Journal of Monetary Economics* 21:35–46.

Engle, R. F., and C. W. Granger. 1987. Co-integration and error correction: Representation, estimation, and testing. *Econometrica* 251–76.

Evans, G. W. 1991. Pitfalls in testing for explosive bubbles in asset prices. *The American Economic Review* 81:922–30.

Evripidou, A. C., D. I. Harvey, S. J. Leybourne, and R. Sollis. 2022. Testing for co-explosive behaviour in financial time series. *Oxford Bulletin of Economics and Statistics* 84:624–50.

Fama, E. F. 1984. Forward and spot exchange rates. *Journal of Monetary Economics* 14:319–38.

Flood, R. P., and R. J. Hodrick. 1990. On testing for speculative bubbles. *Journal of Economic Perspectives* 4:85–101.

Fuller, W. A. 2009. *Introduction to statistical time series*. John Wiley & Sons.

Granger, C. W. 1969. Prediction with a generalized cost of error function. *Journal of the Operational Research Society* 20:199–207.

Hamilton, J. D., and J. C. Wu. 2014. Risk premia in crude oil futures prices. *Journal of International Money and Finance* 42:9–37.

Harvey, D. I., S. J. Leybourne, R. Sollis, and A. R. Taylor. 2016. Tests for explosive financial bubbles in the presence of non-stationary volatility. *Journal of Empirical Finance* 38:548–74.

Hicks, J. R. 1939. *Value and capital*. Oxford: Oxford University Press.

Hintermann, B., S. Peterson, and W. Rickels. 2016. Price and Market Behavior in Phase II of the EU ETS: A Review of the Literature. *Review of Environmental Economics and Policy* .

Hitzemann, S., and M. Uhrig-Homburg. 2018. Equilibrium price dynamics of emission permits. *Journal of Financial and Quantitative Analysis* 53:1653–78.

Hong, H., G. A. Karolyi, and J. A. Scheinkman. 2020. Climate finance. *The Review of Financial Studies* 33:1011–23.

Jeszke, R., and S. Lizak. 2021. Reflections on the Mechanisms to Protect Against Formation of Price Bubble in the EU ETS Market. *Environmental Protection and Natural Resources* 32:8–17.

Keynes, J. M. 1930. *A treatise on money, vol II*. London: MacMillan.

Kling, C., and J. Rubin. 1997. Bankable permits for the control of environmental pollution. *Journal of Public Economics* 64:101–15.

Koch, N., S. Fuss, G. Grosjean, and O. Edenhofer. 2014. Causes of the EU ETS price drop: Recession, CDM, renewable policies or a bit of everything? – New evidence. *Energy Policy* 73:676–85.

Kostakis, A., T. Magdalinos, and M. P. Stamatogiannis. 2015. Robust econometric inference for stock return predictability. *The Review of Financial Studies* 28:1506–53.

Kwiatkowski, D., P. C. Phillips, P. Schmidt, and Y. Shin. 1992. Testing the null hypothesis of stationarity against the alternative of a unit root: How sure are we that economic time series have a unit root? *Journal of Econometrics* 54:159–78.

Liu, R. Y. 1988. Bootstrap procedures under some non-iid models. *The Annals of Statistics* 16:1696–708.

Mammen, E. 1993. Bootstrap and wild bootstrap for high dimensional linear models. *The Annals of Statistics* 21:255–85.

Martinsson, G., P. Strömberg, L. Sajtos, and C. J. Thomann. 2023. The effect of carbon pricing on firm emissions: Evidence from the Swedish CO2 tax. *Review of Financial Studies* .

Montgomery, W. D. 1972. Markets in licenses and efficient pollution control programs. *Journal of Eonomic Theory* 5:395–418.

Newey, W. K., and K. D. West. 1994. Automatic lag selection in covariance matrix estimation. *The Review of Economic Studies* 61:631–53.

OECD. 2018. *Effective carbon rates 2018*.

Pahle, M., C. Günther, S. Osorio, and S. Quemin. 2023. The emerging endgame: The EU ETS on the road towards climate neutrality. *Available at SSRN* .

Pavlidis, E., A. Yusupova, I. Paya, D. Peel, E. Martínez-García, A. Mack, and V. Grossman. 2016. Episodes of exuberance in housing markets: in search of the smoking gun. *The Journal of Real Estate Finance and Economics* 53:419–49.

Pavlidis, E. G., I. Paya, and D. A. Peel. 2017. Testing for speculative bubbles using spot and forward prices. *International Economic Review* 58:1191–226.

———. 2018. Using market expectations to test for speculative bubbles in the crude oil market. *Journal of Money, Credit and Banking* 50:833–56.

Phillips, P. C., and T. Magdalinos. 2007. Limit theory for moderate deviations from a unit root. *Journal of Econometrics* 136:115–30.

———. 2009. Econometric inference in the vicinity of unity. *Singapore Management University, CoFie Working Paper* 7.

Phillips, P. C., and S. Shi. 2020. Real time monitoring of asset markets: Bubbles and crises. In *Handbook of Statistics*, vol. 42, 61–80. Elsevier.

Phillips, P. C., S. Shi, and J. Yu. 2015a. Testing for multiple bubbles: Historical episodes of exuberance and collapse in the S&P 500. *International Economic Review* 56:1043–78.

———. 2015b. Testing for multiple bubbles: Limit theory of real-time detectors. *International Economic Review* 56:1079–134.

Phillips, P. C., and J. Yu. 2011. Dating the timeline of financial bubbles during the subprime crisis. *Quantitative Economics* 2:455–91.

Quemin, S., and M. Pahle. 2023. Financials threaten to undermine the functioning of emissions markets. *Nature Climate Change* 13:22–31.

Rickels, W., D. Görlich, and S. Peterson. 2015. Explaining European emission allowance price dynamics: Evidence from Phase II. *German Economic Review* 16:181–202.

Rubin, J. D. 1996. A model of intertemporal emission trading, banking, and borrowing. *Journal of Environmental Economics and Management* 31:269–86.

Seifert, J., M. Uhrig-Homburg, and M. Wagner. 2008. Dynamic behavior of CO2 spot prices. *Journal of Environmental Economics and Management* 56:180–94.

Stambaugh, R. F. 1999. Predictive regressions. *Journal of Financial Economics* 54:375–421.

Taschini, L. 2021. Flexibility premium of emissions permits. *Journal of Economic Dynamics and Control* 126:104013–.

Tirole, J. 1985. Asset bubbles and overlapping generations. *Econometrica* 53:1499–528.

Trück, S., and R. Weron. 2016. Convenience yields and risk premiums in the EU-ETS – evidence from the Kyoto commitment period. *Journal of Futures Markets* 36:587–611.

Vasilopoulos, K., and E. Pavlidis. 2020. *ivx: Robust econometric inference*. R package version 1.1.0.

Vasilopoulos, K., E. Pavlidis, and E. Martínez-García. 2022. exuber: Recursive right-tailed unit root testing with R. *Journal of Statistical Software* 103:1–26.

Wei, Y., Y. Li, and Z. Wang. 2022. Multiple price bubbles in global major emission trading schemes: Evidence from European Union, New Zealand, South Korea and China. *Energy Economics* 113:106232–.

Yang, B., W. Long, L. Peng, and Z. Cai. 2020. Testing the predictability of us housing price index returns based on an IVX-AR model. *Journal of the American Statistical Association* 115:1598–619.

ZEW. 2019. *Energiemarktbarometer*.

Zhao, J. 2003. Irreversible abatement investment under cost uncertainties: tradable emission permits and emissions charges. *Journal of Public Economics* 87:2765–89. ISSN 0047-2727.

Appendix A: Derivation of $\beta_{1,n}$ and $\beta_{2,n}$ in the presence or absence of a rational bubble

In this section we present the derivation of $\beta_{1,n}$ and $\beta_{2,n}$ under a non-zero risk premium and in the presence or absence of an ongoing rational bubble.

We assume that the fundamental evolves following a mildly explosive process, viz. $U_t = \theta U_{t-1} + \vartheta_t$, where $\theta = 1 + c \times T^{-\alpha}$ with $c > 0$ and $\alpha \in (0,1)$, as detailed in Phillips and Magdalinos (2007), and that fundamental and bubble component are uncorrelated. Further note that fundamental and bubble component are uncorrelated with future innovations, i.e.,

$$\begin{aligned} \operatorname{Cov}(\vartheta_{t+n}, U_t) = \quad & \operatorname{Cov}(\vartheta_{t+n}, B_t) = \quad \operatorname{Cov}\left(\vartheta_{t+n}, RP_{n,t}\right) \\ = \operatorname{Cov}(\epsilon_{t+n}, U_t) = \quad & \operatorname{Cov}(\epsilon_{t+n}, B_t) = \quad \operatorname{Cov}\left(\epsilon_{t+n}, RP_{n,t}\right) = 0. \end{aligned}$$

Consider the slope coefficients of FPR 1 and FPR 2, i.e.,

$$\beta_{1,n} := \frac{\operatorname{Cov}\left(F_{n,t} - P_{t+n}, F_{n,t} - P_t\right)}{\operatorname{Var}\left(F_{n,t} - P_t\right)} \qquad \text{and} \qquad \beta_{2,n} := \frac{\operatorname{Cov}\left(P_{t+n} - P_t, F_{n,t} - P_t\right)}{\operatorname{Var}\left(F_{n,t} - P_t\right)}.$$

Under the above assumption, we obtain the numerator of $\beta_{1,n}$ as

$$\begin{aligned} & \operatorname{Cov}\left(F_{n,t} - P_{t+n}, F_{n,t} - P_t\right) \\ & = \operatorname{Cov}\left(-\vartheta_{t+n} - (1+\rho)^n \left(\frac{1}{\pi^n} - 1\right) B_t - \epsilon_{t+n} + RP_{n,t}, (\theta^n - 1) U_t + ((1+\rho)^n - 1) B_t + RP_{n,t}\right) \\ & = \operatorname{Var}\left(RP_{n,t}\right) - \underbrace{(1+\rho)^n \left(\frac{1}{\pi^n} - 1\right)((1+\rho)^n - 1)}_{=:\gamma_{1,n}} \operatorname{Var}(B_t) - (1+\rho)^n \left(\frac{1}{\pi^n} - 1\right)(\theta^n - 1) \underbrace{\operatorname{Cov}(B_t, U_t)}_{=0} \\ & + \underbrace{\left(2(1+\rho)^n - \left(\frac{1+\rho}{\pi}\right)^n - 1\right)}_{=:\gamma_{2,n}} \operatorname{Cov}\left(B_t, RP_{n,t}\right) + \underbrace{(\theta^n - 1) \operatorname{Cov}\left(U_t, RP_{n,t}\right)}_{\to 0 \text{ as } T \to \infty} \\ & - (\theta^n - 1) \underbrace{\operatorname{Cov}(\vartheta_{t+n}, U_t)}_{=0} - ((1+\rho)^n - 1) \underbrace{\operatorname{Cov}(\vartheta_{t+n}, B_t)}_{=0} - \underbrace{\operatorname{Cov}\left(\vartheta_{t+n}, RP_{n,t}\right)}_{=0} \\ & - (\theta^n - 1) \underbrace{\operatorname{Cov}(\epsilon_{t+n}, U_t)}_{=0} - ((1+\rho)^n - 1) \underbrace{\operatorname{Cov}(\epsilon_{t+n}, B_t)}_{=0} - \underbrace{\operatorname{Cov}\left(\epsilon_{t+n}, RP_{n,t}\right)}_{=0}, \end{aligned}$$

and the numerator of $\beta_{2,n}$ as

$$
\begin{aligned}
&\operatorname{Cov}\left(P_{t+n}-P_t, F_{n,t}-P_t\right)\\
&=\operatorname{Cov}\left((\theta^n-1)U_t+\vartheta_{t+n}+\left(\left(\frac{1+\rho}{\pi}\right)^n-1\right)B_t+\epsilon_{t+n}, (\theta^n-1)U_t+((1+\rho)^n-1)B_t+RP_{n,t}\right)\\
&=\underbrace{\left(\left(\frac{1+\rho}{\pi}\right)^n-1\right)((1+\rho)^n-1)}_{=:\gamma_{3,n}}\operatorname{Var}(B_t)+\underbrace{(\theta^n-1)^2\operatorname{Var}(U_t)}_{\to 0 \text{ as } T\to\infty}\\
&+\underbrace{\left(\left(\frac{1+\rho}{\pi}\right)^n-1\right)}_{=:\gamma_{4,n}}\operatorname{Cov}\left(B_t, RP_{n,t}\right)+\underbrace{(\theta^n-1)\operatorname{Cov}\left(U_t, RP_{n,t}\right)}_{\to 0 \text{ as } T\to\infty}\\
&+(\theta^n-1)\underbrace{\operatorname{Cov}(\vartheta_{t+n}, U_t)}_{=0}+((1+\rho)^n-1)\underbrace{\operatorname{Cov}(\vartheta_{t+n}, B_t)}_{=0}+\underbrace{\operatorname{Cov}\left(\vartheta_{t+n}, RP_{n,t}\right)}_{=0}\\
&+(\theta^n-1)\underbrace{\operatorname{Cov}(\epsilon_{t+n}, U_t)}_{=0}+((1+\rho)^n-1)\underbrace{\operatorname{Cov}(\epsilon_{t+n}, B_t)}_{=0}+\underbrace{\operatorname{Cov}\left(\epsilon_{t+n}, RP_{n,t}\right)}_{=0}.
\end{aligned}
$$

For the denominator of $\beta_{1,n}$ and of $\beta_{2,n}$, we receive

$$
\begin{aligned}
&\operatorname{Var}\left(F_{n,t}-P_t\right)=\operatorname{Var}\left(RP_{n,t}+(\theta^n-1)U_t+((1+\rho)^n-1)B_t\right)\\
&=\operatorname{Var}\left(RP_{n,t}\right)+\underbrace{((1+\rho)^n-1)^2}_{=:\gamma_n^2}\operatorname{Var}(B_t)+\underbrace{(\theta^n-1)^2\operatorname{Var}(U_t)}_{\to 0 \text{ as } T\to\infty}\\
&+2\underbrace{((1+\rho)^n-1)}_{=:\gamma_n}\operatorname{Cov}\left(B_t, RP_{n,t}\right)+2\underbrace{(\theta^n-1)\operatorname{Cov}\left(U_t, RP_{n,t}\right)}_{\to 0 \text{ as } T\to\infty}.
\end{aligned}
$$

This gives us

$$
\beta_{1,n}=\frac{\operatorname{Var}\left(RP_{n,t}\right)-\gamma_{1,n}\operatorname{Var}(B_t)+\gamma_{2,n}\operatorname{Cov}\left(B_t, RP_{n,t}\right)}{\operatorname{Var}\left(RP_{n,t}\right)+\gamma_n^2\operatorname{Var}(B_t)+2\gamma_n\operatorname{Cov}\left(B_t, RP_{n,t}\right)} \qquad \text{for} \qquad T\to\infty
$$

and

$$
\beta_{2,n}=\frac{\gamma_{3,n}\operatorname{Var}(B_t)+\gamma_{4,n}\operatorname{Cov}\left(B_t, RP_{n,t}\right)}{\operatorname{Var}\left(RP_{n,t}\right)+\gamma_n^2\operatorname{Var}(B_t)+2\gamma_n\operatorname{Cov}\left(B_t, RP_{n,t}\right)} \qquad \text{for} \qquad T\to\infty.
$$

Appendix B: Tables and Figures

Table 1: Size

			FPR							KPSS			
λ	T	α	0.7	0.75	0.8	0.85	λ	T	α	0.7	0.75	0.8	0.85
0	150		0.06	0.05	0.06	0.05	0	150		0.04	0.05	0.05	0.04
	300		0.05	0.05	0.05	0.05		300		0.05	0.04	0.05	0.05
0.5	150		0.05	0.05	0.05	0.06	0.5	150		0.08	0.08	0.08	0.08
	300		0.05	0.05	0.05	0.05		300		0.08	0.08	0.08	0.07
1	150		0.06	0.05	0.05	0.05	1	150		0.90	0.91	0.91	0.90
	300		0.06	0.06	0.05	0.05		300		0.97	0.97	0.97	0.97
1.01	150		0.07	0.06	0.06	0.05	1.01	150		0.96	0.96	0.96	0.95
	300		0.09	0.06	0.05	0.05		300		0.99	0.99	0.99	0.99
ϱ	T	α	0.7	0.75	0.8	0.85	ϱ	T	α	0.7	0.75	0.8	0.85
−0.01	150		0.05	0.05	0.06	0.05	−0.01	150		0.31	0.19	0.14	0.11
	300		0.05	0.05	0.05	0.05		300		0.70	0.44	0.30	0.21
+0.01	150		0.05	0.05	0.05	0.06	+0.01	150		0.31	0.21	0.15	0.11
	300		0.05	0.05	0.05	0.05		300		0.67	0.46	0.31	0.22

Explanations: The table displays the rejection rates given that $B_t = 0$ of the Wald statistic based on FPR 2 for the null that $\beta_{2,n} = 0$ (left panel), as well as the rejection rates of the KPSS for the null that $P_{t+1} - F_{1,t}$ is stationary (right panel). The nominal size is fixed at 5%, and we conduct 10,000 replications. The upper panels correspond to the scenario where $\text{Cov}\left(U_t, RP_{n,t}\right) = 0$, and the lower panel corresponds to the case where $\text{Cov}\left(U_t, RP_{n,t}\right) = \varrho\theta\,\text{Var}\left(U_t\right) \neq 0$. The underlying fundamental process is characterized by explosiveness, with a parameter $c = 0.1$ and varying α; λ controls the persistence of the risk premium.

Table 2: Estimation of $\beta_{2,n}$

λ	π	0.3	0.5	0.7	0.9
	$\beta_{2,n}$	26.67	12.00	5.71	2.22
0	Mean	26.67	12.00	5.71	2.22
	SD	1×10^{-14}	4×10^{-15}	2×10^{-15}	8×10^{-14}
ϱ	π	0.3	0.5	0.7	0.9
	$\beta_{2,n}$	29.96	13.48	6.42	2.50
-0.01	Mean	29.96	13.48	6.42	2.50
	SD	2×10^{-14}	6×10^{-15}	3×10^{-15}	9×10^{-14}
	$\beta_{2,n}$	24.02	10.81	5.15	2.00
$+0.01$	Mean	24.02	10.81	5.15	2.00
	SD	1×10^{-14}	5×10^{-15}	2×10^{-15}	7×10^{-14}

Explanations: The table displays the mean (denoted by Mean) and standard deviation (denoted by SD) of IVX estimates for $\beta_{2,n}$ based on 10,000 simulated price paths of a non-collapsing bubble process (DGP B 1) with $\rho = 0.1$ and $\pi \in \{0.3, 0.5, 0.7, 0.9\}$ and the risk premium is generated by DGP RP 1 (upper panel) and by DGP RP 3 (lower panel). We examine the case where $\lambda = 0$, meaning the risk premium is stationary, and ϱ takes values from the set $\{-0.01, +0.01\}$.

Table 3: Estimation of $\beta_{2,n}$ (cont'd)

Blanchard							Evans						
λ	T	π	0.3	0.5	0.7	0.9	λ	T	π	0.3	0.5	0.7	0.9
0	150	Mean	−2.54	−2.41	−2.10	−1.47	0	150	Mean	−5.67	−4.94	−3.68	−1.85
		SD	2.59	2.00	1.39	0.80			SD	2.34	1.45	0.98	0.91
	300	Mean	−2.90	−2.71	−2.33	−1.64		300	Mean	−6.42	−5.30	−3.76	−1.86
		SD	2.53	1.93	1.25	0.59			SD	1.66	0.91	0.69	0.65
0.5	150	Mean	−2.27	−2.21	−1.95	−1.43	0.5	150	Mean	−5.43	−4.76	−3.60	−1.82
		SD	2.51	2.00	1.41	0.82			SD	2.27	1.48	0.96	0.95
	300	Mean	−2.60	−2.53	−2.20	−1.59		300	Mean	−6.16	−5.17	−3.71	−1.86
		SD	2.47	1.94	1.29	0.63			SD	1.58	0.97	0.71	0.64
1	150	Mean	−0.92	−0.97	−0.95	−0.94	1	150	Mean	−2.72	−2.70	−2.40	−1.59
		SD	1.77	1.59	1.27	0.87			SD	2.57	2.01	1.38	0.93
	300	Mean	−0.79	−0.85	−0.91	−1.04		300	Mean	−2.83	−2.84	−2.54	−1.73
		SD	1.71	1.47	1.22	0.81			SD	2.53	1.96	1.24	0.64
1.01	150	Mean	−0.71	−0.73	−0.74	−0.82	1.01	150	Mean	−2.20	−2.16	−1.98	−1.50
		SD	1.65	1.43	1.16	0.88			SD	2.45	2.08	1.46	0.91
	300	Mean	−0.32	−0.37	−0.41	−0.65		300	Mean	−1.28	−1.36	−1.37	−1.35
		SD	1.08	1.04	0.91	0.78			SD	2.05	1.81	1.41	0.78
ϱ	T	π	0.3	0.5	0.7	0.9	ϱ	T	π	0.3	0.5	0.7	0.9
−0.01	150	Mean	−2.59	−2.54	−2.19	−1.61	−0.01	150	Mean	−6.12	−5.34	−4.03	−2.09
		SD	2.88	2.28	1.56	0.91			SD	2.68	1.69	1.15	1.01
	300	Mean	−3.03	−2.85	−2.50	−1.79		300	Mean	−6.99	−5.83	−4.18	−2.09
		SD	2.80	2.14	1.43	0.71			SD	1.70	1.02	0.75	0.75
+0.01	150	Mean	−2.42	−2.33	−2.03	−1.37	+0.01	150	Mean	−5.35	−4.59	−3.37	−1.67
		SD	2.38	1.82	1.23	0.71			SD	1.86	1.17	0.88	0.85
	300	Mean	−2.80	−2.63	−2.21	−1.49		300	Mean	−5.96	−4.85	−3.41	−1.68
		SD	2.27	1.70	1.10	0.54			SD	1.16	0.77	0.63	0.59

Explanations: The table displays the mean (denoted by Mean) and standard deviation (denoted by SD) of IVX estimates for $\beta_{2,n}$ based on 10,000 simulated price paths of a collapsing bubble process and the risk premium is generated by DGP RP 1 (upper panel) and by DGP RP 3 (lower panel). The simulations use the DGPs B 2 (left panel) and B 3 (right panel) with $\rho = 0.1$ and π values from the set $\{0.3, 0.5, 0.7, 0.9\}$.

Table 4: Power

FPR							GSADF						
λ	T	π	0.3	0.5	0.7	0.9	λ	T	π	0.3	0.5	0.7	0.9
0	150		0.71	0.75	0.80	0.89	0	150		0.31	0.33	0.32	0.40
	300		0.88	0.90	0.94	0.98		300		0.47	0.50	0.48	0.59
0.5	150		0.64	0.69	0.77	0.88	0.5	150		0.30	0.34	0.33	0.42
	300		0.84	0.89	0.93	0.97		300		0.47	0.51	0.50	0.61
1	150		0.25	0.32	0.38	0.58	1	150		0.31	0.35	0.34	0.41
	300		0.30	0.36	0.46	0.74		300		0.46	0.50	0.49	0.61
1.01	150		0.19	0.23	0.28	0.50	1.01	150		0.31	0.34	0.33	0.43
	300		0.12	0.15	0.21	0.47		300		0.49	0.53	0.52	0.63
ϱ	T	π	0.3	0.5	0.7	0.9	ϱ	T	π	0.3	0.5	0.7	0.9
−0.01	150		0.68	0.73	0.78	0.88	−0.01	150		0.30	0.33	0.31	0.41
	300		0.85	0.89	0.93	0.97		300		0.47	0.50	0.49	0.61
+0.01	150		0.73	0.78	0.84	0.91	+0.01	150		0.31	0.32	0.32	0.39
	300		0.90	0.93	0.95	0.98		300		0.46	0.49	0.47	0.57

Explanations: The table presents rejection rates for $B_t > 0$ whereas the bubble is generated by Blanchard's DGP B 2 and the risk premium is generated by DGP RP 1 (upper panel) and by DGP RP 3 (lower panel). The left panel shows the rejection rates of a Wald statistic based on FPR 2, while the right panel illustrates the rejection rates of the GSADF test applied to $P_{t+1} - F_{1,t}$. The nominal size is set at 5%, and we perform 10,000 replications. The underlying fundamental process follows a random walk.

Table 5: Power (cont'd)

FPR							GSADF						
λ	T	π	0.3	0.5	0.7	0.9	λ	T	π	0.3	0.5	0.7	0.9
0	150		0.99	1.00	0.99	0.98	0	150		0.57	0.56	0.54	0.51
	300		1.00	1.00	1.00	0.99		300		0.75	0.69	0.66	0.61
0.5	150		0.99	1.00	0.99	0.98	0.5	150		0.57	0.56	0.52	0.50
	300		1.00	1.00	1.00	0.99		300		0.74	0.69	0.66	0.62
1	150		0.72	0.79	0.86	0.94	1	150		0.57	0.55	0.54	0.51
	300		0.85	0.91	0.96	0.99		300		0.74	0.68	0.65	0.60
1.01	150		0.55	0.63	0.72	0.88	1.01	150		0.57	0.56	0.54	0.52
	300		0.41	0.49	0.61	0.87		300		0.71	0.67	0.65	0.60
ϱ	T	π	0.3	0.5	0.7	0.9	ϱ	T	π	0.3	0.5	0.7	0.9
−0.01	150		0.99	1.00	0.99	0.98	−0.01	150		0.57	0.56	0.54	0.53
	300		1.00	1.00	1.00	0.99		300		0.75	0.69	0.66	0.65
+0.01	150		1.00	1.00	0.99	0.98	+0.01	150		0.57	0.55	0.52	0.45
	300		1.00	1.00	1.00	0.99		300		0.75	0.69	0.64	0.56

Explanations: The table presents rejection rates for $B_t > 0$ whereas the bubble is generated by Evans' DGP B 3 and the risk premium is generated by DGP RP 1 (upper panel) and by DGP RP 3 (lower panel). The left panel shows the rejection rates of a Wald statistic based on FPR 2, while the right panel illustrates the rejection rates of the GSADF test applied to $P_{t+1} - F_{1,t}$. The nominal size is set at 5%, and we perform 10,000 replications. The underlying fundamental process follows a random walk.

Table 6: Testing explosiveness of EU ETS spot and futures rates

	Lags	P_t	$F_{4,t}$	$F_{8,t}$	$F_{12,t}$	$F_{16,t}$
SADF	1	4.96^r	4.97^r	4.98^r	4.97^r	4.96^r
	4	5.43^r	5.45^r	5.46^r	5.45^r	5.43^r
GSADF	1	4.96^r	4.97^r	4.98^r	4.97^r	4.97^r
	4	5.43^r	5.45^r	5.46^r	5.45^r	5.43^r

Explanations: The table presents the test statistics of the SADF and GSADF test applied to the spot and futures rates. Superscript r indicates rejection at the 5% significance level whereas critical values are obtained by bootstrapping with 999 repetitions.

Table 7: Testing a bubble in the EU ETS by the FPR approach

		Third and fourth trading period			
	n	4	8	12	16
OLS	$\hat{\beta}_{2,n}$	−1.86	−1.50	−1.90	−1.68
	$\lvert t_\beta \rvert$	0.86	1.61	3.00^r	3.35^r
		(0.39)	(0.11)	(0.00)	(0.00)
IVX	$\hat{\beta}_{2,n}$	−1.59	−1.30	−1.84	−1.70
	W_β	0.54	1.91	8.01^r	11.09^r
		(0.46)	(0.17)	(0.00)	(0.00)
IVX-AR	$\hat{\beta}_{2,n}$	−2.84	−2.14	−1.59	−2.00
	$\widetilde{W}_\beta$	3.05	2.45	1.72	2.34
		(0.08)	(0.12)	(0.19)	(0.13)
	W_{AR}	329.9^r	556.6^r	860.2^r	833.7^r
		(0.00)	(0.00)	(0.00)	(0.00)

Explanations: Estimates for the slope coefficient $\hat{\beta}_{2,n}$ of FPR 2 for the full-sample (January 2018 to October 2023). The slope coefficients are estimated by Ordinary Least Squares, by the IVX estimator according to Kostakis, Magdalinos, and Stamatogiannis (2015) and by the IVX-AR estimator according to Yang, Long, Peng, and Cai (2020). The absolute value of the t-statistic in the OLS case is denoted by $|t_\beta|$ and the values of the Wald statistic is denoted by W_β for the approach by Kostakis, Magdalinos, and Stamatogiannis (2015) and by $\widetilde{W}_\beta$ for the approach by Yang, Long, Peng, and Cai (2020). Further, W_{AR} denotes the Wald statistic for the joint hypothesis that all included lags in the error term of FPR 2 are equal to zero. We use the BIC to select the lag length. Superscript r indicates rejection at the 5% significance level and p—values are in parentheses.

Table 8: Testing a bubble in the EU ETS by the FPR approach (cont'd)

		Third trading period			
	n	4	8	12	16
OLS	$\hat{\beta}_{2,n}$	−19.54	−0.53	−9.86	−4.61
	$\lvert t_\beta \rvert$	1.47	0.08	2.33^r	1.36
		(0.14)	(0.94)	(0.02)	(0.18)
IVX	$\hat{\beta}_{2,n}$	−18.07	5.09	−3.81	1.99
	W_β	1.85	0.54	0.73	0.29
		(0.17)	(0.46)	(0.39)	(0.59)
IVX-AR	$\hat{\beta}_{2,n}$	−8.15	−0.35	−5.72	−0.24
	$\widetilde{W}_\beta$	1.57	0.01	2.10	0.01
		(0.21)	(0.91)	(0.15)	(0.94)
	W_{AR}	350.9^r	805.0^r	641.6^r	1071.0^r
		(0.00)	(0.00)	(0.00)	(0.00)

		Fourth trading period			
	n	4	8	12	16
OLS	$\hat{\beta}_{2,n}$	−3.38	−3.30	−3.78	−3.64
	$\lvert t_\beta \rvert$	1.03	2.22^r	3.80^r	4.70^r
		(0.31)	(0.03)	(0.00)	(0.00)
IVX	$\hat{\beta}_{2,n}$	−2.62	−2.80	−3.70	−3.63
	W_β	0.62	3.42	13.02^r	20.64^r
		(0.43)	(0.06)	(0.00)	(0.00)
IVX-AR	$\hat{\beta}_{2,n}$	−1.92	−1.76	−2.61	−3.05
	$\widetilde{W}_\beta$	0.52	0.93	2.51	2.93
		(0.47)	(0.33)	(0.11)	(0.09)
	W_{AR}	195.5^r	697.5^r	593.4^r	563.9^r
		(0.00)	(0.00)	(0.00)	(0.00)

Explanations: Estimates for the slope coefficient $\hat{\beta}_{2,n}$ of FPR 2 for the sub-samples (January 2018 to December 2021 in the left panel and January 2022 to October 2023 in the right panel). The slope coefficients are estimated by Ordinary Least Squares, by the IVX estimator according to Kostakis, Magdalinos, and Stamatogiannis (2015) and by the IVX-AR estimator according to Yang, Long, Peng, and Cai (2020). The absolute value of the t-statistic in the OLS case is denoted by $|t_\beta|$ and the values of the Wald statistic is denoted by W_β for the approach by Kostakis, Magdalinos, and Stamatogiannis (2015) and by $\widetilde{W}_\beta$ for the approach by Yang, Long, Peng, and Cai (2020). Further, W_{AR} denotes the Wald statistic for the joint hypothesis that all included lags in the error term of FPR 2 are equal to zero. We use the BIC to select the lag length. Superscript r indicates rejection at the 5% significance level and p—values are in parentheses.

Table 9: Testing a bubble in the EU ETS by the GSADF approach

	Lags n	4	8	12	16
SADF	1	−4.24	−2.38	−1.11	−1.13
	4	−1.26	−0.76	−0.34	−0.36
GSADF	1	−0.17	0.67	1.52	1.68
	4	1.07	2.02	1.59	2.22

Explanations: The table presents the test statistics of the SADF and GSADF test applied to the differential between future spot rates and futures rates with $n \in \{4, 8, 12, 16\}$ weeks. Superscript r indicates rejection at the 5% significance level whereas critical values are obtained by bootstrapping with 999 repetitions.

Table 10: Testing a bubble in the EU ETS by the KPSS-type approach

Third and fourth trading period				
n	4	8	12	16
Bootstrap CV 5%	0.138	0.139	0.153	0.167
Test statistic	0.248^r	0.254^r	0.296^r	0.327^r

Explanations: Bootstrap CV 5% denotes the 5% critical value for the testing procedure for co-explosiveness obtained by wild bootstrap and the row below contains the test statistic for the full sample (January 2018 to October 2023). We reject $\mathscr{H}_0$ at the 5% significance level if the test statistic is larger than the bootstrap critical value (indicated by superscript r).

Table 11: Testing a bubble in the EU ETS by the KPSS-type approach (cont'd)

Third trading period					Fourth trading period				
n	4	8	12	16	n	4	8	12	16
Bootstrap CV 5%	0.347	0.400	0.367	0.433	Bootstrap CV 5%	0.282	0.248	0.210	0.190
Test statistic	0.227	0.176	0.145	0.155	Test statistic	0.168	0.115	0.121	0.108

Explanations: Bootstrap CV 5% denotes the 5% critical value for the testing procedure for co-explosiveness obtained by wild bootstrap and the row below contains the test statistic for the sub-sample (January 2018 to December 2021 in the left panel and January 2022 to October 2023 in the right panel). We reject $\mathscr{H}_0$ at the 5% significance level if the test statistic is larger than the bootstrap critical value (indicated by superscript r).

Figure 1: Spot price series of emission allowances in the EU ETS

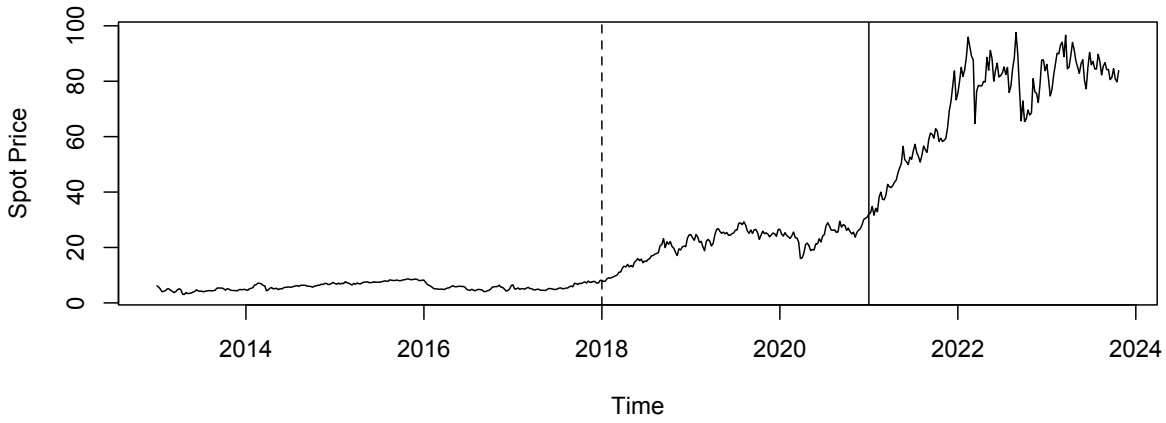

Explanations: The dotted vertical line indicates the (supposed) start of the price surge (2018). The solid vertical line indicates the start of the fourth trading period (2021).

Figure 2: Timing of explosiveness in EU ETS spot and futures prices

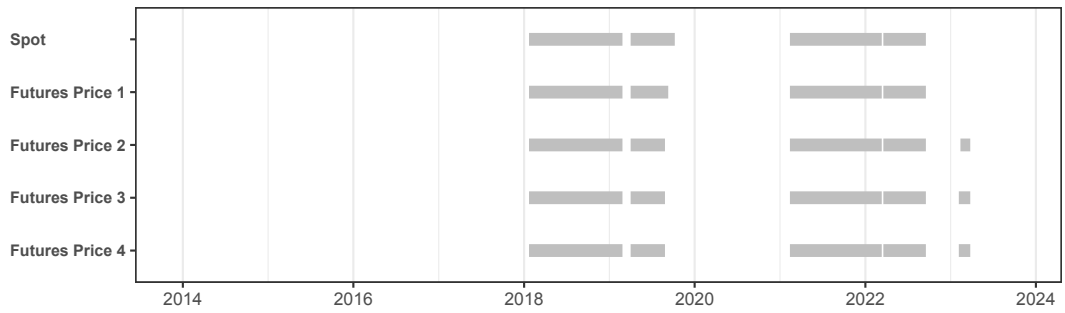

Explanations: The regions shaded in gray signify explosive periods, as determined by the BSADF procedure at a 5% significance level, employing one lag and a minimum window size of 36 observations. "Spot" denotes the date stamping for the spot price, while "Futures Price 1" corresponds to the futures price with delivery in one month (4 weeks), and so forth.

Figure 3: Timing of explosiveness in EU ETS spot and futures prices (cont'd)

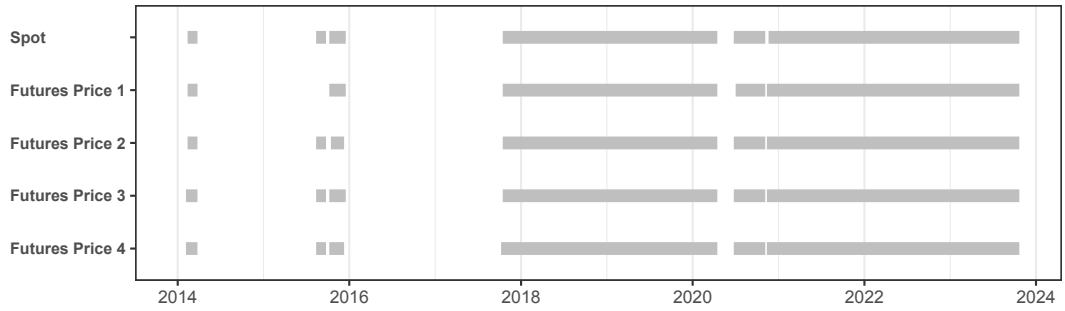

Explanations: The regions shaded in gray signify explosive periods, as determined by the BSADF procedure at a 5% significance level, employing four lag and a minimum window size of 36 observations. "Spot" denotes the date stamping for the spot price, while "Futures Price 1" corresponds to the futures price with delivery in one month (4 weeks), and so forth.

Appendix C: Further Monte Carlo Studies

In this section, we present supplementary findings from simulation studies regarding the power to identify rational bubbles of the Fama Predictive Regression (FPR) approach, in particular FPR 2, and the Generalized Supremum Augmented Dickey Fuller (GSADF) test applied to $P_{t+n} - F_{n,t}$, where n takes values from the set $2, 3, 4$. In particular, we consider $P_t = U_t + B_t$ and $F_{n,t} = \mathbb{E}_t[P_{t+n}] + RP_{n,t}$ whereas

(i) the fundamental is generated by a random walk, i.e., $U_t = U_{t-1} + \vartheta_t$ with $U_0 = 100$ and $\vartheta_t \sim$ i.i.d.$N(0,1)$,

(ii) the bubble is generated by DGP B 2 (see Table 12 to Table 14) and by DGP B 3 (see Table 15 to Table 17), respectively,

(iii) the risk premium is generated by $RP_{n,t} = \lambda RP_{n,t-1} + \varphi_t$ with $\lambda \in \{0, 0.5, 1, 1.01\}$ (upper panel in the following tables) and $RP_{n,t} = \varrho \times (1+\rho) B_t + \varrho \times \theta U_t + \varphi_t$ with $\varrho \in \{-0.01, +0.01\}$ where $\varphi_t \sim$ i.i.d. $N(0,1)$ (lower panel in the following tables),

(iv) the sample size takes on values from the set $T \in \{150, 300\}$.

We note a constant power level in the GSADF approach for extended forecast horizons, whereas the power of the FPR approach shows an upward trend in all examined scenarios below. This phenomenon can be attributed to the growing persistence in the regressand in FPR 2 for longer predictive horizons, especially when a rational bubble is present. Regarding our specific application, it is noteworthy that as n exceeds one, the evidence against the price being influenced by a rational bubble becomes increasingly compelling.

Table 12: Power with $n = 2$ (Blanchard)

FPR						GSADF					
λ	T	π	0.3	0.5	0.7	0.9	λ	T	π	0.3	0.5	0.7	0.9
0	150		0.87	0.92	0.94	0.97	0	150		0.36	0.44	0.44	0.51
	300		0.97	0.98	0.99	0.99		300		0.55	0.62	0.63	0.69
0.5	150		0.84	0.89	0.93	0.97	0.5	150		0.38	0.46	0.45	0.52
	300		0.96	0.98	0.99	0.99		300		0.57	0.64	0.64	0.71
1	150		0.42	0.56	0.66	0.82	1	150		0.38	0.45	0.45	0.54
	300		0.51	0.64	0.74	0.91		300		0.55	0.63	0.63	0.71
1.01	150		0.31	0.42	0.51	0.71	1.01	150		0.38	0.44	0.45	0.54
	300		0.23	0.29	0.38	0.66		300		0.58	0.66	0.67	0.75
ϱ	T	π	0.3	0.5	0.7	0.9	ϱ	T	π	0.3	0.5	0.7	0.9
−0.01	150		0.85	0.92	0.94	0.97	−0.01	150		0.36	0.44	0.45	0.52
	300		0.97	0.98	0.99	0.99		300		0.55	0.63	0.62	0.71
+0.01	150		0.88	0.93	0.95	0.97	+0.01	150		0.36	0.43	0.43	0.50
	300		0.98	0.99	0.99	0.99		300		0.55	0.63	0.63	0.69

Explanations: The table presents rejection rates for $B_t > 0$ and $n = 2$ whereas the bubble is generated by Blanchard's DGP B 2 and the risk premium is generated by DGP RP 1 (upper panel) and by DGP RP 3 (lower panel). The left panel shows the rejection rates of a Wald statistic based on FPR 2, while the right panel illustrates the rejection rates of the GSADF test applied to $P_{t+2} - F_{2,t}$. The nominal size is set at 5%, and we perform 10,000 replications. The underlying fundamental process follows a random walk.

Table 13: Power with $n = 3$ (Blanchard)

FPR							GSADF						
λ	T	π	0.3	0.5	0.7	0.9	λ	T	π	0.3	0.5	0.7	0.9
0	150		0.92	0.95	0.97	0.98	0	150		0.37	0.47	0.49	0.57
	300		0.99	0.99	0.99	0.99		300		0.55	0.67	0.69	0.75
0.5	150		0.90	0.93	0.96	0.98	0.5	150		0.38	0.49	0.52	0.59
	300		0.98	0.99	0.99	0.99		300		0.56	0.68	0.70	0.77
1	150		0.55	0.67	0.79	0.91	1	150		0.39	0.49	0.51	0.59
	300		0.65	0.78	0.86	0.96		300		0.55	0.68	0.70	0.78
1.01	150		0.43	0.55	0.65	0.82	1.01	150		0.39	0.49	0.50	0.61
	300		0.31	0.39	0.49	0.75		300		0.60	0.71	0.74	0.81
ϱ	T	π	0.3	0.5	0.7	0.9	ϱ	T	π	0.3	0.5	0.7	0.9
−0.01	150		0.91	0.95	0.97	0.98	−0.01	150		0.37	0.46	0.49	0.57
	300		0.99	0.99	0.99	0.99		300		0.55	0.66	0.70	0.77
+0.01	150		0.93	0.96	0.98	0.98	+0.01	150		0.36	0.47	0.48	0.57
	300		0.99	1.00	1.00	1.00		300		0.55	0.66	0.69	0.75

Explanations: The table presents rejection rates for $B_t > 0$ and $n = 3$ whereas the bubble is generated by Blanchard's DGP B 2 and the risk premium is generated by DGP RP 1 (upper panel) and by DGP RP 3 (lower panel). The left panel shows the rejection rates of a Wald statistic based on FPR 2, while the right panel illustrates the rejection rates of the GSADF test applied to $P_{t+3} - F_{3,t}$. The nominal size is set at 5%, and we perform 10,000 replications. The underlying fundamental process follows a random walk.

Table 14: Power with $n = 4$ (Blanchard)

FPR							GSADF						
λ	T	π	0.3	0.5	0.7	0.9	λ	T	π	0.3	0.5	0.7	0.9
0	150		0.94	0.96	0.97	0.98	0	150		0.35	0.48	0.53	0.60
	300		0.99	0.99	0.99	0.99		300		0.53	0.67	0.73	0.79
0.5	150		0.92	0.94	0.97	0.98	0.5	150		0.37	0.49	0.54	0.63
	300		0.98	0.99	0.99	0.99		300		0.54	0.69	0.73	0.81
1	150		0.63	0.74	0.84	0.95	1	150		0.36	0.50	0.54	0.62
	300		0.74	0.84	0.91	0.98		300		0.55	0.69	0.73	0.81
1.01	150		0.51	0.63	0.74	0.88	1.01	150		0.37	0.50	0.55	0.63
	300		0.40	0.48	0.57	0.82		300		0.58	0.73	0.78	0.85
ϱ	T	π	0.3	0.5	0.7	0.9	ϱ	T	π	0.3	0.5	0.7	0.9
−0.01	150		0.94	0.96	0.97	0.98	−0.01	150		0.36	0.48	0.53	0.62
	300		0.99	0.99	0.99	0.99		300		0.52	0.69	0.72	0.80
+0.01	150		0.95	0.97	0.98	0.98	+0.01	150		0.35	0.48	0.52	0.60
	300		0.99	1.00	1.00	0.99		300		0.54	0.68	0.72	0.79

Explanations: The table presents rejection rates for $B_t > 0$ and $n = 4$ whereas the bubble is generated by Blanchard's DGP B 2 and the risk premium is generated by DGP RP 1 (upper panel) and by DGP RP 3 (lower panel). The left panel shows the rejection rates of a Wald statistic based on FPR 2, while the right panel illustrates the rejection rates of the GSADF test applied to $P_{t+4} - F_{4,t}$. The nominal size is set at 5%, and we perform 10,000 replications. The underlying fundamental process follows a random walk.

Table 15: Power with $n = 2$ (Evans)

FPR							GSADF						
λ	T	π	0.3	0.5	0.7	0.9	λ	T	π	0.3	0.5	0.7	0.9
0	150		1.00	1.00	0.99	0.98	0	150		0.56	0.64	0.67	0.75
	300		1.00	1.00	1.00	0.99		300		0.75	0.80	0.80	0.83
0.5	150		1.00	1.00	0.99	0.98	0.5	150		0.57	0.64	0.67	0.74
	300		1.00	1.00	1.00	0.99		300		0.75	0.80	0.81	0.83
1	150		0.93	0.96	0.98	0.98	1	150		0.56	0.64	0.67	0.74
	300		0.97	0.99	0.99	0.99		300		0.75	0.80	0.81	0.84
1.01	150		0.79	0.85	0.91	0.96	1.01	150		0.58	0.65	0.67	0.74
	300		0.62	0.71	0.81	0.96		300		0.72	0.80	0.79	0.83
ϱ	T	π	0.3	0.5	0.7	0.9	ϱ	T	π	0.3	0.5	0.7	0.9
−0.01	150		0.93	0.97	0.98	0.98	−0.01	150		0.57	0.63	0.67	0.75
	300		0.98	0.99	1.00	0.99		300		0.74	0.81	0.81	0.83
+0.01	150		0.93	0.96	0.98	0.98	+0.01	150		0.57	0.64	0.67	0.75
	300		0.98	0.99	0.99	0.99		300		0.74	0.80	0.80	0.83

Explanations: The table presents rejection rates for $B_t > 0$ and $n = 2$ whereas the bubble is generated by Evans' DGP B 3 and the risk premium is generated by DGP RP 1 (upper panel) and by DGP RP 3 (lower panel). The left panel shows the rejection rates of a Wald statistic based on FPR 2, while the right panel illustrates the rejection rates of the GSADF test applied to $P_{t+2} - F_{2,t}$. The nominal size is set at 5%, and we perform 10,000 replications. The underlying fundamental process follows a random walk.

Table 16: Power with $n = 3$ (Evans)

FPR							GSADF						
λ	T	π	0.3	0.5	0.7	0.9	λ	T	π	0.3	0.5	0.7	0.9
0	150		1.00	1.00	1.00	0.99	0	150		0.56	0.66	0.71	0.80
	300		1.00	1.00	1.00	1.00		300		0.74	0.83	0.85	0.88
0.5	150		1.00	1.00	0.99	0.99	0.5	150		0.57	0.65	0.71	0.80
	300		1.00	1.00	1.00	0.99		300		0.73	0.82	0.86	0.88
1	150		0.98	0.99	0.99	0.98	1	150		0.56	0.66	0.72	0.80
	300		1.00	1.00	1.00	1.00		300		0.73	0.82	0.85	0.88
1.01	150		0.89	0.94	0.96	0.98	1.01	150		0.55	0.65	0.72	0.80
	300		0.74	0.83	0.91	0.98		300		0.70	0.83	0.85	0.89
ϱ	T	π	0.3	0.5	0.7	0.9	ϱ	T	π	0.3	0.5	0.7	0.9
−0.01	150		0.98	0.99	0.99	0.98	−0.01	150		0.56	0.66	0.72	0.80
	300		0.99	1.00	1.00	0.99		300		0.73	0.83	0.85	0.88
+0.01	150		0.98	0.99	0.99	0.99	+0.01	150		0.56	0.66	0.71	0.80
	300		0.99	1.00	1.00	0.99		300		0.72	0.82	0.85	0.88

Explanations: The table presents rejection rates for $B_t > 0$ and $n = 3$ whereas the bubble is generated by Evans' DGP B 3 and the risk premium is generated by DGP RP 1 (upper panel) and by DGP RP 3 (lower panel). The left panel shows the rejection rates of a Wald statistic based on FPR 2, while the right panel illustrates the rejection rates of the GSADF test applied to $P_{t+3} - F_{3,t}$. The nominal size is set at 5%, and we perform 10,000 replications. The underlying fundamental process follows a random walk.

Table 17: Power with $n = 4$ (Evans)

			FPR							GSADF				
λ	T	π	0.3	0.5	0.7	0.9	λ	T	π	0.3	0.5	0.7	0.9
0	150		1.00	1.00	0.99	0.98	0	150		0.55	0.64	0.73	0.82
	300		1.00	1.00	1.00	0.99		300		0.71	0.81	0.87	0.90
0.5	150		1.00	1.00	0.99	0.98	0.5	150		0.55	0.64	0.73	0.82
	300		1.00	1.00	1.00	0.99		300		0.72	0.81	0.87	0.91
1	150		0.99	0.99	0.99	0.99	1	150		0.55	0.64	0.73	0.82
	300		1.00	1.00	1.00	0.99		300		0.71	0.81	0.87	0.90
1.01	150		0.94	0.97	0.98	0.98	1.01	150		0.54	0.63	0.74	0.81
	300		0.82	0.90	0.95	0.99		300		0.68	0.81	0.86	0.90
ϱ	T	π	0.3	0.5	0.7	0.9	ϱ	T	π	0.3	0.5	0.7	0.9
−0.01	150		0.99	0.99	0.99	0.98	−0.01	150		0.54	0.65	0.74	0.82
	300		1.00	1.00	1.00	0.99		300		0.71	0.82	0.87	0.91
+0.01	150		0.99	0.99	0.99	0.99	+0.01	150		0.55	0.64	0.73	0.81
	300		1.00	1.00	1.00	1.00		300		0.71	0.81	0.87	0.90

Explanations: The table presents rejection rates for $B_t > 0$ and $n = 4$ whereas the bubble is generated by Evans' DGP B 3 and the risk premium is generated by DGP RP 1 (upper panel) and by DGP RP 3 (lower panel). The left panel shows the rejection rates of a Wald statistic based on FPR 2, while the right panel illustrates the rejection rates of the GSADF test applied to $P_{t+4} - F_{4,t}$. The nominal size is set at 5%, and we perform 10,000 replications. The underlying fundamental process follows a random walk.